



**HAL**  
open science

## Chiral halogenated Schiff base compounds: green synthesis, anticancer activity and DNA-binding study

Mahnaz Ariyaeifar, Hadi Amiri Rudbari, Mehdi Sahihi, Zahra Kazemi, Abolghasem Abbasi Kajani, Hassan Zali-Boeini, Nazanin Kordestani, Giuseppe Bruno, Sajjad Gharaghani

### ► To cite this version:

Mahnaz Ariyaeifar, Hadi Amiri Rudbari, Mehdi Sahihi, Zahra Kazemi, Abolghasem Abbasi Kajani, et al.. Chiral halogenated Schiff base compounds: green synthesis, anticancer activity and DNA-binding study. *Journal of Molecular Structure*, 2018, 1161, pp.497-511. 10.1016/j.molstruc.2018.02.042 . hal-04086074

**HAL Id: hal-04086074**

**<https://hal.science/hal-04086074v1>**

Submitted on 1 May 2023

**HAL** is a multi-disciplinary open access archive for the deposit and dissemination of scientific research documents, whether they are published or not. The documents may come from teaching and research institutions in France or abroad, or from public or private research centers.

L'archive ouverte pluridisciplinaire **HAL**, est destinée au dépôt et à la diffusion de documents scientifiques de niveau recherche, publiés ou non, émanant des établissements d'enseignement et de recherche français ou étrangers, des laboratoires publics ou privés.

# Chiral halogenated Schiff base compounds: green synthesis, anticancer activity and DNA-binding study

Mahnaz Ariyaefar <sup>a</sup>, Hadi Amiri Rudbari <sup>a</sup>, Mehdi Sahihi <sup>a</sup>, Zahra Kazemi <sup>a</sup>, Abolghasem Abbasi Kajani <sup>a</sup>, Hassan Zali-Boeini <sup>a</sup>, Nazanin Kordestani <sup>a</sup>, Giuseppe Bruno <sup>b</sup>, Sajjad Gharaghani <sup>c</sup>

<sup>a</sup>

Department of Chemistry, University of Isfahan, Isfahan 81746-73441, Iran

<sup>b</sup>

Department of Chemical, Biological, Pharmaceutical and Environmental Sciences, University of Messina, Viale F. Stagno D'Alcontres 31, 98166 Messina, Italy

<sup>c</sup>

Laboratory of Bioinformatics and Drug Design (LBD), Institute of Biochemistry and Biophysics, University of Tehran, Tehran, Iran

## Abstract

Eight enantiomerically pure halogenated Schiff base compounds were synthesized by reaction of halogenated salicylaldehydes with 3-Amino-1,2-propanediol (*R* or *S*) in water as green solvent at ambient temperature. All compounds were characterized by elemental analyses, NMR (<sup>1</sup>H and <sup>13</sup>C), circular dichroism (CD) and FT-IR spectroscopy. FS-DNA binding studies of these compounds carried out by fluorescence quenching and UV-vis spectroscopy. The obtained results

revealed that the ligands bind to DNA as: (*R* **ClBr**) > (*R* **Cl<sub>2</sub>**) > (*R* **Br<sub>2</sub>**) > (*R* **I<sub>2</sub>**)

and (*S* **ClBr**) > (*S* **Cl<sub>2</sub>**) > (*S* **Br<sub>2</sub>**) > (*S* **I<sub>2</sub>**), indicating the effect of halogen

on binding constant. In addition, DNA-binding constant of the *S* and *R*-enantiomers are different from each other. The ligands can form halogen bonds with DNA that were confirmed by molecular docking. This method was also measured the bond distances and bond angles. The study of obtained data can have concluded that binding affinity of the ligands to DNA depends on strength of halogen bonds. The potential anticancer activity of ligands were also evaluated on MCF-7 and HeLa cancer cell lines by using MTT assay. The results showed that the anticancer activity and FS-DNA interaction is significantly dependent on the stereoisomers of Schiff base compounds as *R*-enantiomers displayed significantly higher activity than *S*-enantiomers. The molecular docking was also used to illustrate the specific DNA-binding of synthesized compounds and groove binding mode of DNA interaction was proposed for them. In addition, molecular

docking results indicated that there are three types of bonds (H and X-bond and hX-bond) between synthesized compounds and base pairs of DNA.

## Keywords

Halogenated Schiff base ligand

DNA binding

Halogen bonding

In vitro assay

## 1. Introduction

Cancer is undoubtedly one of the world's major health issues and several million-people died from this disease every year. In this regard, cisplatin is a promising and well-known metal-based drug for cancer therapy [1]. However, side effects or toxicity of cisplatin and its second-generation analogs made it is an urgent need to develop new drugs with minimal side effects and maximal curative potential [2].

Schiff base ligands and complexes have gained much importance in medicinal chemistry in view of their biological, pharmacological, antitumor activity and their exceptional chelating ability [[3], [4], [5], [6]]. It should be noted that in comparison to Schiff base complexes, literature reports reveal that Schiff base ligands shows less or no cytotoxic activity [7,8].

On the other hand, Chirality is usually a significant factor in the field of pharmaceuticals due to chirality of nucleic acids and the other biomacromolecules such as proteins, enzymes, amino acids, carbohydrates and hormones. Furthermore, researches confirm that chirality improves the pharmacological behavior of compounds [9], and each of enantiomerically pure molecules may therefore lead to different diastereomeric interactions with DNA [10]. Cancer cells were preliminary cultured.

Halogens have been classically incorporated into the development of pharmaceuticals to increase membrane permeability and decrease metabolic degradation [11]. There is now a greater appreciation that halogens play a direct role in the efficacy of certain drugs through a molecular interaction that is defined as the halogen bond or X-bonds (Fig. 1) [12].

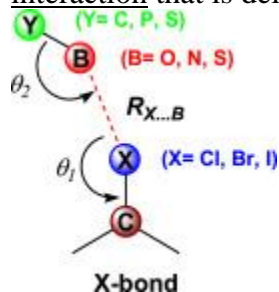


Fig. 1. The X-bond is defined as a short, directional interaction between a halogen substituent (X) and an electron-rich acceptor atom (B). The approach of the acceptor to the halogen and halogen to the acceptor are labeled as  $\theta_1$  and  $\theta_2$ , respectively. The interactions are characterized by a halogen-to-base distance  $R_{X...B}$  that is shorter than the sum of their respective van der Waals radii.

A halogen bond in biomolecules can be referred to a short  $C-X\cdots B$  Y interaction, where B Y is a halogen bond donor, C-X is a carbon-bonded chlorine, bromine, or iodine; B Y is a carbonyl, hydroxyl, thiol, aromatic ring, charged carboxylate, phosphate group, or amine, and the  $X\cdots B$  distance is less than or equal to the sums of the respective van der Waals radii.

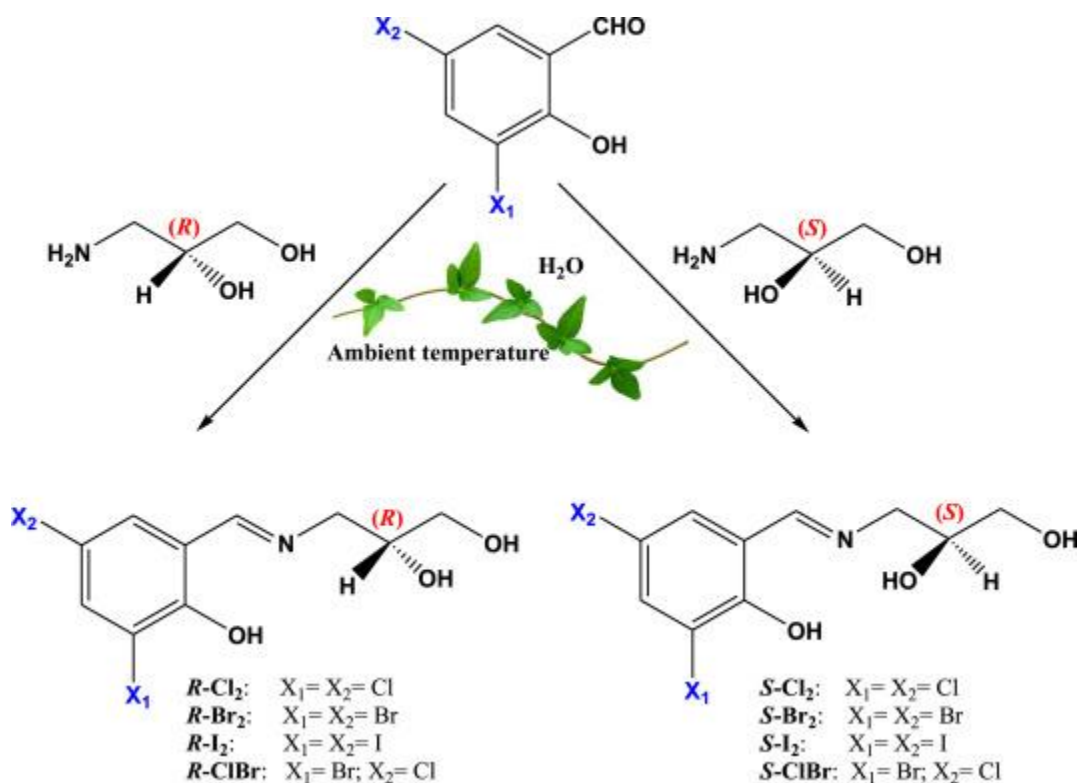
X-bonding often provide several orders of magnitude in specificity and affinity of inhibitors toward their molecular targets. Although fluorine is the better substituent, the percent of fluorinated compounds decreases whereas those of the heavier halogens (Cl, Br, and I) that most commonly form X-bonds increase from 40% at the start to >60% of halogenated drugs at launch [13]. Thus, there is enormous potential to exploit X-bonding as a molecular tool in medicinal chemistry if the interaction can be accurately incorporated into drug design algorithms.

As in the literature reported, the most common synthetic route for synthesis Schiff bases is the reaction of aldehydes and ketones with primary amines. The reaction is generally carried out by refluxing the carbonyl compounds and amines in organic solvents by separating water as formed with an azeotroping agent or by anhydrous Na<sub>2</sub>SO<sub>4</sub> and MgSO<sub>4</sub> [[14], [15], [16], [17], [18]]. The replacement of volatile organic solvents in organic reaction processes is an important green chemistry goal. Among the green solvents, use of water as a biodegradable, nonflammable and readily available resource is attractive [19,20]. However, due to lack of stability of imine bonds in water, less attention has been focused on the synthesis of Schiff base ligands and complexes in water as solvent.

According to the above mentioned important factors in design and synthesis of anticancer compounds and also in embracing the principles of green chemistry, herein we reported synthesis

of eight chiral halogenated Schiff base compounds, **R** **Cl<sub>2</sub>**, **R** **Br<sub>2</sub>**, **R** **I<sub>2</sub>**, **R**

**ClBr**, **S** **Cl<sub>2</sub>**, **S** **Br<sub>2</sub>**, **S** **I<sub>2</sub>** and **S** **ClBr**, from condensation of halogenated salicylaldehydes with enantiomerically pure 3-Amino-1,2-propanediol (*R* or *S*) in water as green solvent at ambient temperature with high yield (more than 90%) and purity (Scheme 1). The compounds were characterized by elemental analyses, NMR (<sup>1</sup>H and <sup>13</sup>C) and FT-IR spectroscopies. During this study, a comparative study between biological activities of **R**- and **S**-halogenated ligands have been carried out. In addition, the effect of halogens on biological activities of the ligands have been investigated. Therefore, their DNA-binding have been evaluated by means of both experimental (fluorescence quenching and UV-Vis spectroscopy methods) and computational methods (molecular docking). The synthesized ligands have been also screened for their *in vitro* anti-proliferative activities against human cell lines (MCF-7 and HeLa).



Scheme 1. Synthesis of chiral halogenated Schiff base compounds.

## 2. Experimental

### 2.1. Chemicals and instrumentation

RPMI-1640 medium, Fetal bovine serum (FBS), Dimethyl sulfoxide (DMSO), antibiotics (penicillin-streptomycin) solution, and 3-(4,5-Dimethylthiazol-2-yl)-2,5-Diphenyltetrazolium Bromide (MTT) were purchased from Sigma (Germany).

Fish sperm DNA (FS-DNA), Tris(hydroxymethyl)-aminomethane (Tris), ethidium bromide (3,8-diamino-5-ethyl-6-phenylphenanthridinium bromide, EthBr), 3,5-dibromosalicylaldehyde, 3,5-diiodosalicylaldehyde, 3,5-dichlorosalicylaldehyde, 3-Bromo-5-chlorosalicylaldehyde, (*R*)-3-Amino-1,2-propanediol and (*S*)-3-Amino-1,2-propanediol were purchased from Sigma-Aldrich and used without further purification. All salts used for buffer preparation were analytical grade and were dissolved in double distilled water. All of the solutions were used freshly after preparation.

The FT-IR spectrum was recorded on a JASCO, FT/IR-6300 spectrometer ( $4000\text{--}400\text{ cm}^{-1}$ ) in KBr pellets.  $^1\text{H}$  and  $^{13}\text{C}$  NMR spectra were recorded on a Bruker Avance III 400 spectrometer using DMSO. The elemental analysis was performed on Leco, CHNS-932 and Perkin-Elmer 7300 DV elemental analyzers. The UV-Vis spectra were recorded on a Perkin-Elmer LAMBDA 265 spectrophotometer. Fluorescence measurements were carried out on Shimadzu RF-5000 spectrofluorometer at room temperature.

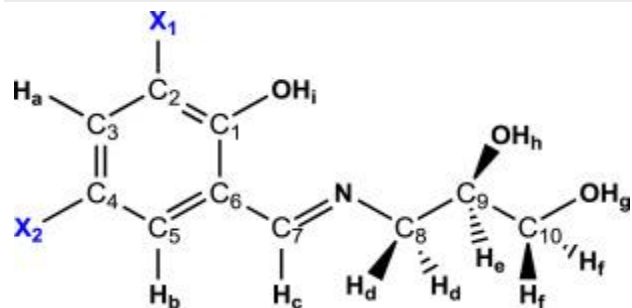
## 2.2. Synthesis of Schiff base compounds

All chiral Schiff base compounds were synthesized using identical reaction conditions, therefore only the synthesis of *R* Cl<sub>2</sub> will be described in detail. The addition of 10 mmol of 3,5-dichlorosalicylaldehyde to a distilled water solution (20 mL) of (*R*)-3-Amino-1,2-propanediol (10 mmol) at room temperature yielded a yellow precipitate almost immediately. The reaction mixture was stirred for overnight, then the yellow precipitate was collected by filtration, washed with 50 mL of distilled water, and dried in air.

*R* Cl<sub>2</sub>: Yield 93%, M.p = 128 °C, Anal. Calc. for C<sub>10</sub>H<sub>11</sub>Cl<sub>2</sub>NO<sub>3</sub>: C, 45.48; H, 4.20; N, 5.30;

Found: C, 45.53; H, 4.21; N, 5.34. FT-IR (KBr, cm<sup>-1</sup>): 3141–3327 (ν<sub>O-H</sub>, br, vs), 1657 (ν<sub>C=N</sub>). <sup>1</sup>HNMR and <sup>13</sup>CNMR (DMSO-d<sub>6</sub>, 400 MHz, 298 K): Table 1.

Table 1. <sup>1</sup>H NMR and <sup>13</sup>C NMR data of Schiff base compounds with tetramethylsilane, TMS, as internal standard (chemical shifts in ppm and *J* in Hz).



<sup>1</sup>HNMR

	<i>R</i> I <sub>2</sub>	<i>R</i> Br <sub>2</sub>	<i>R</i> Cl <sub>2</sub>	<i>R</i> ClBr (X <sub>1</sub> :Br; X <sub>2</sub> :Cl)
H <sub>a</sub>	8.00 (d, 1H, <i>J</i> = 2.2 Hz)	7.77 (d, 1H, <i>J</i> = 2.6 Hz)	7.55 (d, 1H, <i>J</i> = 2.7 Hz)	7.70 (d, 1H, <i>J</i> = 2.7 Hz)
H <sub>b</sub>	7.68 (d, 1H, <i>J</i> = 2.2 Hz)	7.56 (d, 1H, <i>J</i> = 2.6 Hz)	7.41 (d, 1H, <i>J</i> = 2.7 Hz)	7.46 (d, 1H, <i>J</i> = 2.7 Hz)
H <sub>c</sub>	8.40 (d, 1H, <i>J</i> = 8.4 Hz)	8.48 (d, 1H, <i>J</i> = 8.5 Hz)	8.51 (d, 1H, <i>J</i> = 4.6 Hz)	8.49 (d, 1H, <i>J</i> = 4.8 Hz)
H <sub>d</sub>	3.77 (t of d, 1H)	3.76 (t of d, 1H)	3.78 (d of d, 1H, <i>J</i> = 9.8 and 2.9 Hz)	3.79 (d of d, 1H, <i>J</i> = 7.1 and 3.8 Hz)

H <sub>d</sub>	3.54 (m, 1H)	3.54 (m, 1H)	3.54 (d of d, 1H, J = 6.8 and 5.7 Hz)	3.54 (d of d, 1H, J = 6.8 and 5.7 Hz)
H <sub>e</sub>	3.71 (m, 1H)	3.70 (m, 1H)	3.70 (m, 1H)	3.70 (m, 1H)
H <sub>f</sub>	3.43 (m, 1H)	3.42 (m, 1H)	3.43 (m, 1H)	3.43 (m, 1H)
H <sub>f</sub>	3.32 (m, 1H)	3.31 (m, 1H)	3.31 (m, 1H)	3.31 (m, 1H)
H <sub>g</sub>	4.82 (t, 1H, J = 5.5 Hz)	4.82 (t, 1H, J = 5.5 Hz)	4.82 (t, 1H, J = 5.1 Hz)	4.82 (t, 1H, J = 5.3 Hz)
H <sub>h</sub>	5.16 (d, 1H, J = 4.5 Hz)	5.17 (d, 1H, J = 5.0 Hz)	5.16 (d, 1H, J = 4.9 Hz)	5.16 (d, 1H, J = 5.0 Hz)
H <sub>i</sub>	14.62 (s, 1H)	14.63 (s, 1H)	14.63 (s, 1H)	14.68 (s, 1H)
	<i>S</i> I <sub>2</sub>	<i>S</i> Br <sub>2</sub>	<i>S</i> Cl <sub>2</sub>	<i>S</i> ClBr (X <sub>1</sub> :Br; X <sub>2</sub> :Cl)
H <sub>a</sub>	8.04 (d, 1H, J = 2.2 Hz)	7.84 (d, 1H, J = 2.5 Hz)	7.63 (d, 1H, J = 2.7 Hz)	7.79 (d, 1H, J = 2.7 Hz)
H <sub>b</sub>	7.72 (d, 1H, J = 2.3 Hz)	7.63 (d, 1H, J = 2.5 Hz)	7.49 (d, 1H, J = 2.7 Hz)	7.54 (d, 1H, J = 2.7 Hz)
H <sub>c</sub>	8.44 (d, 1H, J = 8.4 Hz)	8.55 (d, 1H, J = 7.4 Hz)	8.58 (s, 1H)	8.58 (d, 1H, J = 7.6 Hz)
H <sub>d</sub>	3.81 (t of d, 1H)	3.85 (br d, 1H, J = 12.8 Hz)	3.85 (d of d, 1H, J = 9.8 and 2.9 Hz)	3.87 (br d, 1H)
H <sub>d</sub>	3.57 (m, 1H)	3.61 (d of d, 1H, J = 6.8 and 5.1 Hz)	3.61 (d of d, 1H, J = 6.8 and 5.7 Hz)	3.63 (d of d, 1H, J = 7.1 and 3.8 Hz)
H <sub>e</sub>	3.73 (m, 1H)	3.77 (m, 1H)	3.78 (m, 1H)	3.79 (m, 1H)
H <sub>f</sub>	3.45 (m, 1H)	3.50 (m, 1H)	3.48 (m, 1H)	3.52 (m, 1H)
H <sub>f</sub>	3.35 (m, 1H)	3.38 (m, 1H)	3.41 (m, 1H)	3.40 (m, 1H)

H <sub>g</sub>	4.87 (t, 1H, <i>J</i> = 5.6 Hz)	4.89 (t, 1H, <i>J</i> = 5.1 Hz)	4.90 (t, 1H, <i>J</i> = 5.5 Hz)	4.92 (t, 1H, <i>J</i> = 5.5 Hz)
H <sub>h</sub>	5.21 (d, 1H, <i>J</i> = 5.1 Hz)	5.24 (d, 1H, <i>J</i> = 5.3 Hz)	5.24 (d, 1H, <i>J</i> = 5.1 Hz)	5.26 (d, 1H, <i>J</i> = 5.1 Hz)
H <sub>i</sub>	14.65 (s, 1H)	14.70 (s, 1H)	14.70 (s, 1H)	14.76 (s, 1H)

<sup>13</sup>CNMR

	<i>R</i> I <sub>2</sub>	<i>R</i> Br <sub>2</sub>	<i>R</i> Cl <sub>2</sub>	<i>R</i> ClBr	<i>S</i>	I <sub>2</sub>	<i>S</i> Br <sub>2</sub>	<i>S</i> Cl <sub>2</sub>	<i>S</i> ClBr
C <sub>1</sub>	168.27	166.05	164.84	165.44	168.32	166.09	164.91	165.51	
C <sub>2</sub>	73.51	88.24	115.97	115.90	73.51	88.24	115.94	115.96	
C <sub>3</sub>	148.97	138.31	133.00	135.95	148.99	138.33	133.03	134.10	
C <sub>4</sub>	95.76	102.85	125.11	115.96	95.83	102.85	125.14	115.96	
C <sub>5</sub>	141.23	134.25	130.39	131.09	141.26	134.27	130.42	131.13	
C <sub>6</sub>	116.74	116.78	116.31	116.49	116.73	116.78	116.29	116.48	
C <sub>7</sub>	165.98	166.20	166.23	166.20	166.01	166.22	166.25	166.23	
C <sub>8</sub>	55.83	55.93	56.23	56.16	55.81	55.93	56.20	56.15	
C <sub>9</sub>	69.82	69.82	69.85	69.84	69.82	69.81	69.85	69.85	
C <sub>10</sub>	63.17	63.16	63.18	63.18	63.16	63.17	63.18	63.20	

**R Br<sub>2</sub>**: Yield 94%, M.p = 166 °C, Anal. Calc. for C<sub>10</sub>H<sub>11</sub>Br<sub>2</sub>NO<sub>3</sub>: C, 34.02; H, 3.14; N, 3.97;

Found: C, 34.05; H, 3.15; N, 4.01. FT-IR (KBr, cm<sup>-1</sup>): 3163–3333 (ν<sub>O-H</sub>, br, vs), 1656 (ν<sub>C-N</sub>). <sup>1</sup>HNMR and <sup>13</sup>CNMR (DMSO-d<sub>6</sub>, 400 MHz, 298 K): Table 1.



**R I<sub>2</sub>**: Yield 95%, M.p = 172 °C, Anal. Calc. for C<sub>10</sub>H<sub>11</sub>I<sub>2</sub>NO<sub>3</sub>: C, 26.87; H, 2.48; N, 3.13; Found: C, 26.83; H, 2.51; N, 3.15. FT-IR (KBr, cm<sup>-1</sup>): 3216–3363 (ν<sub>O-H</sub>, br, vs), 1651 (ν<sub>C-N</sub>). <sup>1</sup>HNMR and <sup>13</sup>CNMR (DMSO-d<sub>6</sub>, 400 MHz, 298 K): Table 1.

**R ClBr**: Yield 90%, M.p = 149 °C, Anal. Calc. for C<sub>10</sub>H<sub>11</sub>BrClNO<sub>3</sub>: C, 38.93; H, 3.59; N, 4.54; Found: C, 38.90; H, 3.57; N, 4.51. FT-IR (KBr, cm<sup>-1</sup>): 3162–3338 (ν<sub>O-H</sub>, br, vs), 1656 (ν<sub>C-N</sub>). <sup>1</sup>HNMR and <sup>13</sup>CNMR (DMSO-d<sub>6</sub>, 400 MHz, 298 K): Table 1.

**S Cl<sub>2</sub>**: Yield 93%, M.p = 141 °C, Anal. Calc. for C<sub>10</sub>H<sub>11</sub>Cl<sub>2</sub>NO<sub>3</sub>: C, 45.48; H, 4.20; N, 5.30; Found: C, 45.53; H, 4.21; N, 5.34. FT-IR (KBr, cm<sup>-1</sup>): 3140–3326 (ν<sub>O-H</sub>, br, vs), 1658 (ν<sub>C-N</sub>). <sup>1</sup>HNMR and <sup>13</sup>CNMR (DMSO-d<sub>6</sub>, 400 MHz, 298 K): Table 1.

**S Br<sub>2</sub>**: Yield 94%, M.p = 168 °C, Anal. Calc. for C<sub>10</sub>H<sub>11</sub>Br<sub>2</sub>NO<sub>3</sub>: C, 34.02; H, 3.14; N, 3.97; Found: C, 34.05; H, 3.15; N, 4.01. FT-IR (KBr, cm<sup>-1</sup>): 3253–3332 (ν<sub>O-H</sub>, br, vs), 1654 (ν<sub>C-N</sub>). <sup>1</sup>HNMR and <sup>13</sup>CNMR (DMSO-d<sub>6</sub>, 400 MHz, 298 K): Table 1.

**S I<sub>2</sub>**: Yield 95%, M.p = 175 °C, Anal. Calc. for C<sub>10</sub>H<sub>11</sub>I<sub>2</sub>NO<sub>3</sub>: C, 26.87; H, 2.48; N, 3.13; Found: C, 26.83; H, 2.51; N, 3.15. FT-IR (KBr, cm<sup>-1</sup>): 3217–3362 (ν<sub>O-H</sub>, br, vs), 1652 (ν<sub>C-N</sub>). <sup>1</sup>HNMR and <sup>13</sup>CNMR (DMSO-d<sub>6</sub>, 400 MHz, 298 K): Table 1.

**S ClBr**: Yield 90%, M.p = 152 °C, Anal. Calc. for C<sub>10</sub>H<sub>11</sub>BrClNO<sub>3</sub>: C, 38.93; H, 3.59; N, 4.54; Found: C, 38.90; H, 3.57; N, 4.51. FT-IR (KBr, cm<sup>-1</sup>): 3337–3480 (ν<sub>O-H</sub>, br, vs), 1656 (ν<sub>C-N</sub>). <sup>1</sup>HNMR and <sup>13</sup>CNMR (DMSO-d<sub>6</sub>, 400 MHz, 298 K): Table 1.

## 2.3. DNA binding studies

### 2.3.1. Preparation of compounds and DNA stock solutions

The stock solution of FS-DNA was prepared in 50 mM Tris buffer at pH 7.5 using double-distilled deionized water and stored at 4 °C. The FS-DNA concentration per nucleotide was determined using absorption intensity at 260 nm after adequate dilution with the buffer and using the reported molar absorptivity of 6600 M<sup>-1</sup> cm<sup>-1</sup>. Purity of FS-DNA solution was confirmed by ratio of UV absorbance at 260 and 280 nm ( $A_{260}/A_{280} = 1.9$ ), indicating that FS-DNA is free from protein impurity [21]. The solutions of the compounds were first prepared in ethanol as co-solvent, and then diluted with corresponding buffer to the required concentration for all experiments. The volume of co-solvent never exceeded 0.5% (v/v), so the effect of ethanol is negligible. All the solutions were used freshly after preparation.

### **2.3.2. UV-Vis spectroscopy measurements**

Absorption titration experiment as an operational and very easy method was carried out to investigation of DNA-binding of the compounds at room temperature. Absorption spectral titration experiments were performed by addition of various amounts of DNA ( $0-5 \times 10^{-4}$  M) to the compounds ( $1 \times 10^{-4}$  M). All compounds–DNA solutions were allowed to incubate for 2 min before recording the related spectra. Absorption curves of compounds–DNA mixtures were corrected by subtracting the spectra of DNA and all intensities were corrected for the dilution effect.

### **2.3.3. Fluorescence spectroscopic measurements**

In order to carry out fluorescence quenching experiments the FS-DNA solution was stirred with EtBr with molar ratio of DNA-EtBr 10:1 for 1 h at 4 °C. Then, various amounts of ligands (0–250  $\mu$ M) were added to this mixture. The fluorescence spectra were measured in the range of 500–700 nm with exciting wavelength at 520 nm. In each measurement after addition of FS-DNA, the mixture was allowed to stand for 2 min. Moreover, the measured fluorescence intensities were corrected for the dilution and the inner-filter effect.

### **2.3.4. Molecular Docking simulation**

In this work, molecular docking study was carried out to indicate DNA binding site for the synthesized compounds. The optimized structure of the ligands was calculated using Gaussian 09 [22] at the level of B3LYP/6-311G\*\*. The known crystal structure of DNA (PDB ID: 423D) with sequence  $d(\text{ACCGACGTCGGT})_2$  was taken from the Brookhaven Protein Data Bank (<http://www.rcsb.org/pdb>) at resolution of 1.60. The water molecules of the .pdb files were removed and missing hydrogen atoms were added. Flexible-ligand docking was performed by AutoDock 4.2.5.1 molecular-docking program using the implemented empirical free energy function and the Lamarckian Genetic Algorithm [23]. The Gasteiger charges were added to prepare the macromolecule input file for docking and the Auto Grid was used to calculate Grids. For the docking of the ligands with DNA, a docking with 84, 66 and 50 lattice points along X, Y, and Z axes respectively, was performed to find the binding site of the ligands on DNA with a grid point spacing of 0.492 Å. 250 docking runs with 25,000,000 energy evaluations for each run were performed.

### **2.4. In vitro studies of anticancer activity**

MTT assay was used to elucidate the anticancer potential of the compounds on human breast (MCF-7) and cervical (HeLa) cancer cell lines according to the previously reported procedures [24,25]. To this aim, the cancer cells were preliminary cultured in RPMI-1640 medium supplemented with 10% FBS and 1% antibiotics solution and maintained in a humidified 5% CO<sub>2</sub> incubator at 37 °C for two weeks. The cells at a density of  $10^4$  cells per well were subsequently seeded on 96-well plates containing 200  $\mu$ L medium and cultured overnight at the same conditions. After 48 h incubation of the cells with different concentrations (20, 50 and 100  $\mu$ M) of each compound, the medium was removed and 100  $\mu$ L MTT solution ( $0.5 \text{ mg mL}^{-1}$  in media) was added into each well and the plates were incubated again at 37 °C for 4 h. Subsequently, the medium was discarded while the formazan crystals were dissolved in 150  $\mu$ L DMSO and the absorbance was measured at 570 nm. Three independent experiments were conducted for each toxicity endpoint and the results were presented as the mean values obtained from three

independent experiments. The cell viability was determined as ratio of absorbance values from each treatment and the control. The changes in cell morphology following exposure to the corresponding concentrations of the compounds were also monitored by optical microscope to further investigate the anticancer effects of the compounds.

### 3. Results and discussion

#### 3.1. Synthesis and general characterization

Halogenated chiral Schiff base compounds, **R Cl<sub>2</sub>**, **R Br<sub>2</sub>**, **R I<sub>2</sub>**, **S ClBr**,

**S Cl<sub>2</sub>**, **S Br<sub>2</sub>**, **S I<sub>2</sub>** and **S ClBr**, were obtained by the self-condensation reaction between halogenated salicylaldehydes (3,5-dichlorosalicylaldehyde, 3,5-dibromosalicylaldehyde, 3,5-diiodosalicylaldehyde and 3-bromo-5-chlorosalicylaldehyde) with enantiomerically pure 3-amino-1,2-propanediol (*R* or *S*), in distilled water as solvent at ambient temperature (Scheme 1). All compounds were yellow powders, stable in air and moderately soluble in the most common organic solvents such as MeOH, EtOH, CHCl<sub>3</sub>, CH<sub>2</sub>Cl<sub>2</sub>, DMF, DMSO and acetone. The purity and identity of the synthesized ligands were established with the help of elemental analysis, NMR (<sup>1</sup>H and <sup>13</sup>C) and FT-IR spectroscopies. Their spectral and analytical data were in full agreement with the proposed structures.

The formation of Schiff base compounds was evidenced by the presence of strong IR absorption bands at 1657 cm<sup>-1</sup> for **R Cl<sub>2</sub>** and 1658 cm<sup>-1</sup> for **S Cl<sub>2</sub>**, 1655 cm<sup>-1</sup> for **R Br<sub>2</sub>** and 1654 cm<sup>-1</sup> for **S Br<sub>2</sub>**, 1651 cm<sup>-1</sup> for **R I<sub>2</sub>** and 1652 cm<sup>-1</sup> for **S I<sub>2</sub>** and 1656 cm<sup>-1</sup> for **R**

**ClBr** and 1656 cm<sup>-1</sup> for **S ClBr**, due to  $\nu(\text{C}=\text{N})$ , while no bands attributable to C=O or NH<sub>2</sub> were detected. The FT-IR spectra of all Schiff base compounds are shown in figs S1-S8. The presence of several medium intensity bands in the range 2650–3250 cm<sup>-1</sup> suggests the existence of C–H stretching vibrations of aliphatic and aromatic protons. The IR spectra of compounds also exhibit two broad absorption bands in ~3140 and ~3480 cm<sup>-1</sup>, characteristic of the stretching vibration of the phenolic and alcoholic OH groups [26].

The <sup>1</sup>H NMR and <sup>13</sup>C NMR spectra of the title ligands are shown in figs S9-S24. As can be seen, in <sup>1</sup>H NMR spectra a typical signal for the imine functionality **H<sub>c</sub>** were observed between 8 and

9 ppm for all the synthesized compounds. Surprisingly, except compound **S Cl<sub>2</sub>** in all other compounds this characteristic signal was appeared as a doublet peak. It is more likely due to the long range <sup>4</sup>*J* coupling of imine proton with two diastereotopic protons (**H<sub>a</sub>**). As it is predictable, a doublet of doublets signal must be observed for the imine proton, but because of proton exchange a broaden doublet was observed in <sup>1</sup>H NMR spectrum. Beside formation of a Schiff base compound, the possibility of formation of five and/or six-component ring tautomeric mixtures was also reported before [27]. However, as it is explicitly show in <sup>1</sup>H NMR spectrum, appearance of two distinct signals for the both alcoholic OH (a triplet signal at ~4.8 ppm and a doublet at ~5.2 ppm) imply that, the synthesized compounds are only in the form of pure Schiff base. This

is also further demonstrated through comparison of the spectrum with a reported similar structure [28]. As expected, there are also two different multiplets for the vicinal methylenes (diastereotopic) at narrow chemical shifts and between 3.3 and 3.6 ppm regions. In  $^1\text{H}$  NMR spectra of all Schiff base ligands, there is also other characteristic singlet signal resonating at 14–15 ppm region for phenolic (OH, **H<sub>i</sub>**) functional group. The very high chemical shift for the phenolic (OH) proton in the prepared Schiff bases can be ascribed to the intramolecular hydrogen-bonding interaction of this functional group with nitrogen heteroatom of imine functionality. In  $^{13}\text{C}$  NMR spectra of all compounds, there is an intense signal around 164–168 ppm region which is belong to C  $\text{N}$  (**C<sub>7</sub>**) of imine functional group. Very close to this signal there is a weak peak which is related to C

#### O of aromatic ring (**C<sub>1</sub>**).

Electronic circular dichroism (CD) is one of the widely practiced method for determine absolute configurations of chiral molecules [29]. CD is often referred to as the Cotton effect. The Cotton effect is the characteristic change in CD in the vicinity of an absorption band of a substance. In a wavelength region where the light is absorbed, the absolute amplitude of the optical rotation at first varies rapidly with wavelength, crosses zero at absorption maxima and then again varies rapidly with wavelength but in opposite direction. The CD of a chiral molecule is frequency-dependent; measurement of CD over a range of frequencies gives CD spectra. The CD spectra of the two enantiomers of a chiral molecule are of equal magnitude and opposite sign: i.e., mirror-image enantiomers give mirror-image CD spectra [30].

Although it is expected that the CD spectrum of the two enantiomers must be equal magnitude and opposite sign, sometimes factors such as solvent variation, inter- and intramolecular interaction or the presence of a particular substituent in the compounds does not allow the expected spectrum to occur and causes some changes in the CD spectrum [31,32].

CD spectra of the synthesized chiral compounds are shown in Fig. 2. As shown in this figure, enantiomers don't have mirror-image CD spectra. This difference in CD spectra of enantiomers may be due to the possible intramolecular hydrogen bonds in the studied compounds. With

intramolecular hydrogen bonds between nitrogen atom of Schiff base group (C  $\text{N}$ ) and terminal  $\text{OH}$  group, a pseudo-cyclohexane ring can be formed (Fig. 3). With formation of

such ring, the  $\text{OH}$  group of chiral center in *S*-enantiomers is in equatorial position, while in *R*-enantiomers, is in axial position. This two different position for  $\text{OH}$  group of chiral center in two enantiomers cause to creation of other different inter and intramolecular hydrogen bounds in

molecule. As shown in Fig. 3, in *S*-enantiomers, terminal  $\text{OH}$  group can participate in intramolecular hydrogen bonding, while two other  $\text{OH}$  groups (  $\text{OH}$  of chiral center

and  $\text{OH}$  of salicylaldehyde) can participate in intermolecular hydrogen bonding. In other

hand, in *R*-enantiomers, terminal  $\text{OH}$  group and  $\text{OH}$  of salicylaldehyde group can participate in intramolecular hydrogen bonding. It should be noted that the terminal  $\text{OH}$  group

also can participate in intermolecular hydrogen bonding in *R*-enantiomers (Fig. 3). With these proposed structures, we should expect that the melting point of *S*-enantiomers should be more than *R*-enantiomers, because of more intermolecular hydrogen bonding in *S*-enantiomers (two intermolecular hydrogen bonds in *S*-enantiomers and only one intermolecular hydrogen bond in *R*-enantiomers). The results of melting points for *R*- and *S*-enantiomers are in perfect agreement with our proposed structure (see the experimental part). All of *S*-enantiomers have more melting points

than *R*-enantiomers. For example, the melting point for *R* Cl<sub>2</sub> is 128 °C, while for *S* Cl<sub>2</sub> is 141 °C. It should also be noted that the proposed structures for enantiomers are in perfect agreement with our NMR data (Table 1 and electronic supplementary information). As a conclusion, we can say that intermolecular and intramolecular hydrogen bonds cause that the enantiomers have different melting point and CD spectrum.

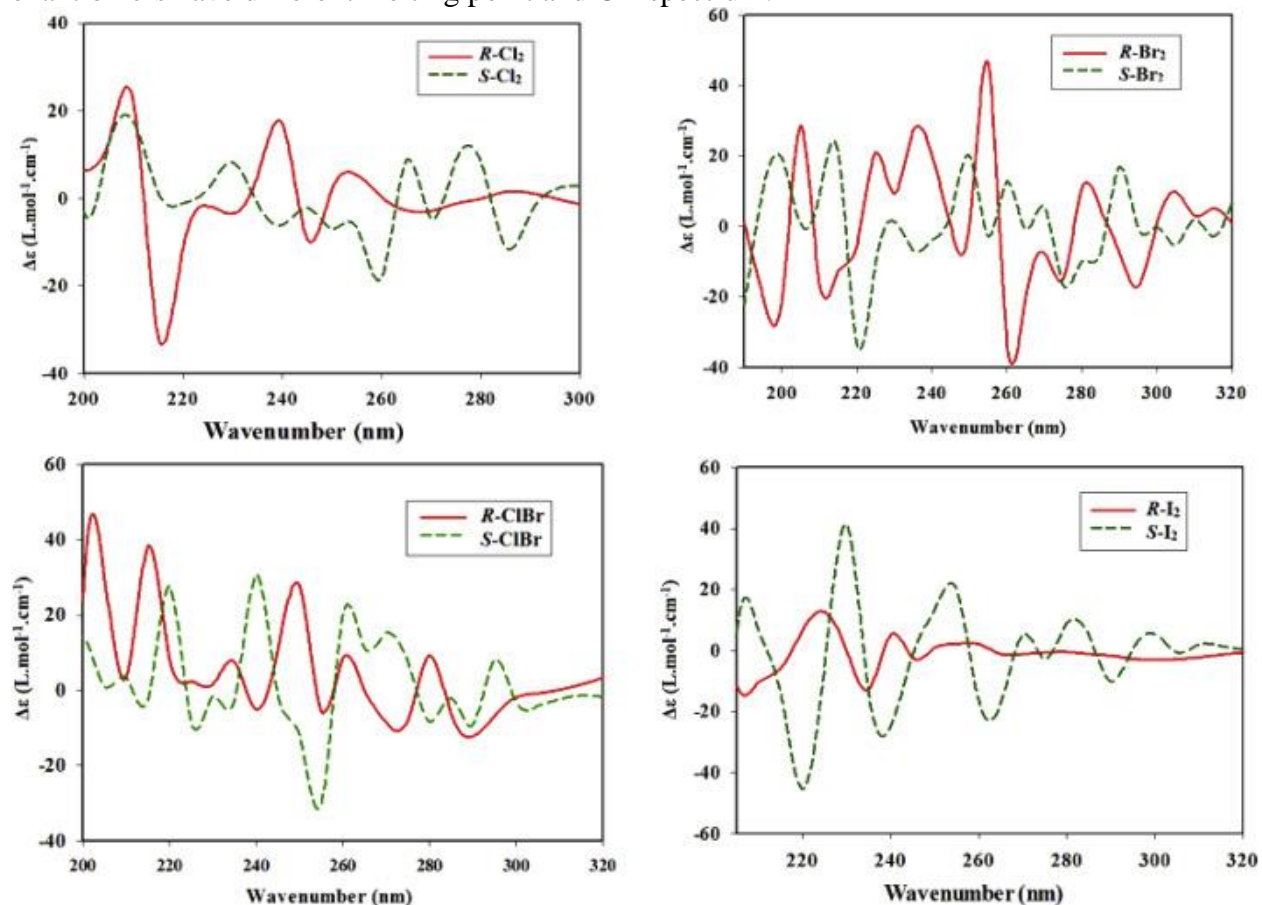


Fig. 2. CD spectra of ligands in ethanol. *R*, *S* Cl<sub>2</sub> (4 mM); *R*, *S* Br<sub>2</sub> (20 mM); *R*, *S* ClBr (20 mM); *R* I<sub>2</sub> (9 mM), *S* I<sub>2</sub> (15 mM).

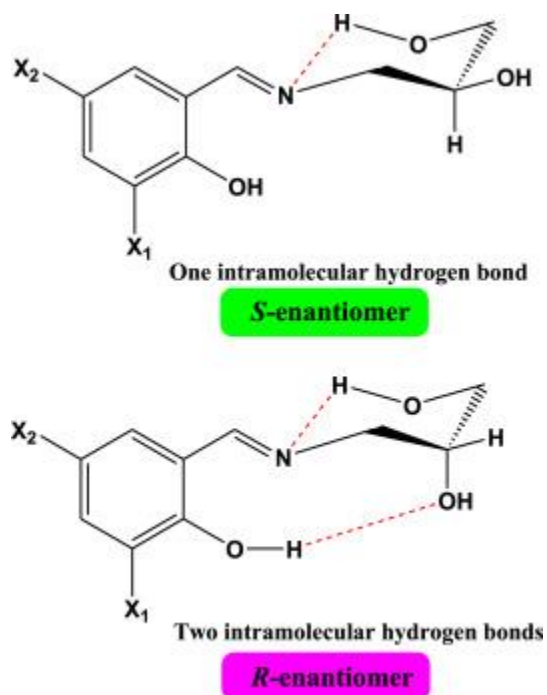


Fig. 3. Formation of intramolecular hydrogen bonding in *S* and *R* enantiomers.

## 3.2. DNA binding properties

### 3.2.1. Absorption spectral studies

Monitoring changes in the absorption spectra of the ligands upon addition of various amounts of DNA is a powerful technique for determining their overall DNA-binding characteristics [33]. Hypochromic and red shift in the UV-Vis spectrum of a drug upon its DNA-binding is indicative of intercalation mode, involving an interaction between  $\pi^*$  orbital of the drug with  $\pi$  orbital of DNA base pairs. Therefore, the probability of electron transition decreases due to the filling of coupled  $\pi^*$ -orbital and so, hypochromic is observed. While a groove binding or electrostatic interaction leads to hyperchromic effect along with blue shift [34,35].

The absorption spectra of the synthesized ligands in the absence and presence of different concentrations of FS-DNA were given in Fig. 4. As shown in this figure, with the addition of FS-DNA a hypochromism in absorption of the ligands was observed. Although, this observation reveals an intercalative mode, some studies reported that this is not a correct conclusion necessarily. The hypochromic effect can be observed as a result of other binding mode such as groove binding due to the changes in the solvent distribution and the orientation effect in moving into the more hydrophobic environment of groove. The structures of the title ligands (Scheme 1) show that they are not planar and therefore, probability of their intercalation is very low. This spectral characteristic suggests that the ligands interact with FS-DNA through the partial insertion of the aromatic rings to the FS-DNA groove [[36], [37], [38]].

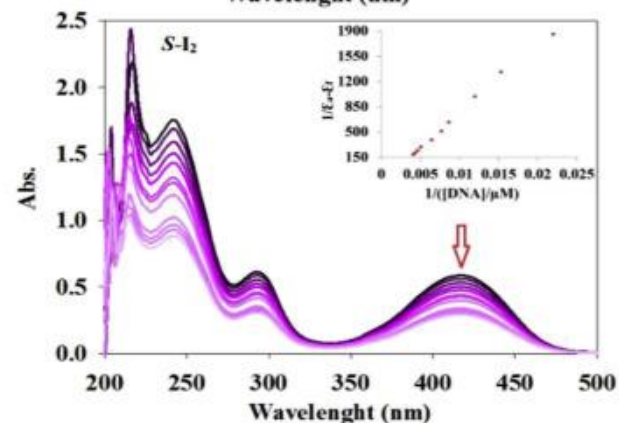
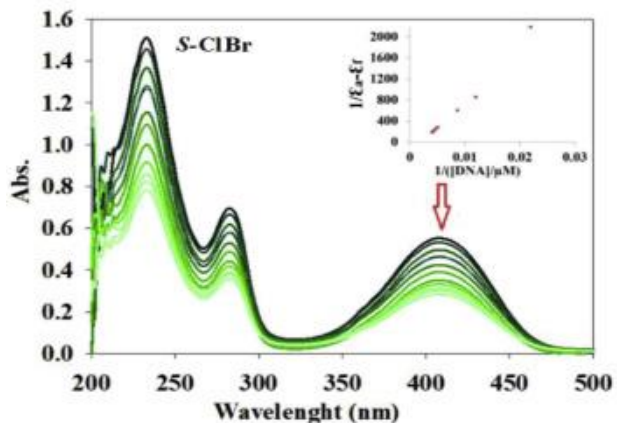
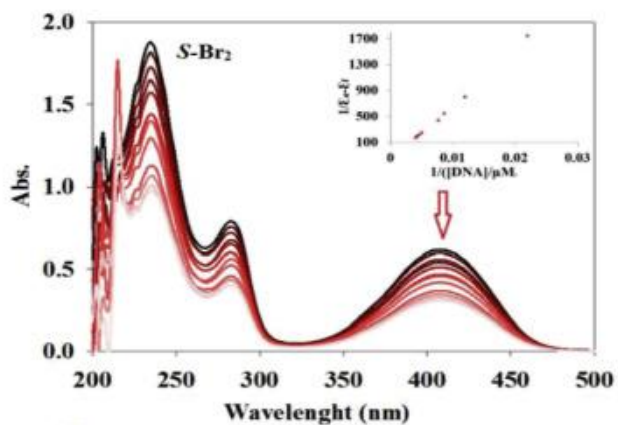
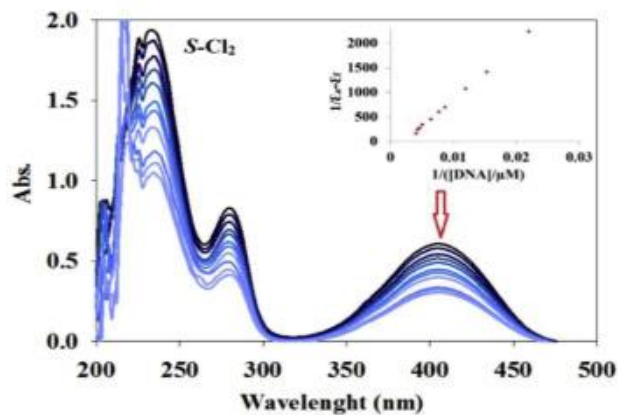
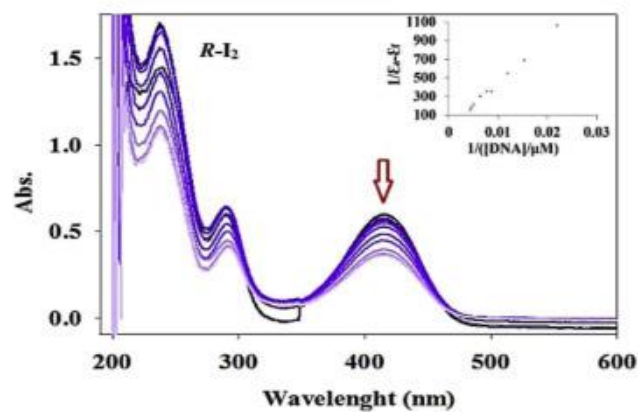
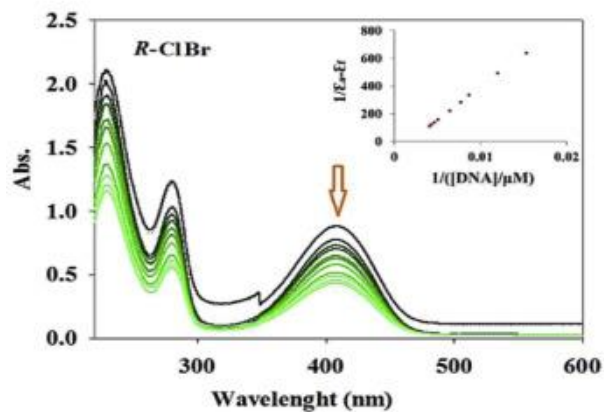
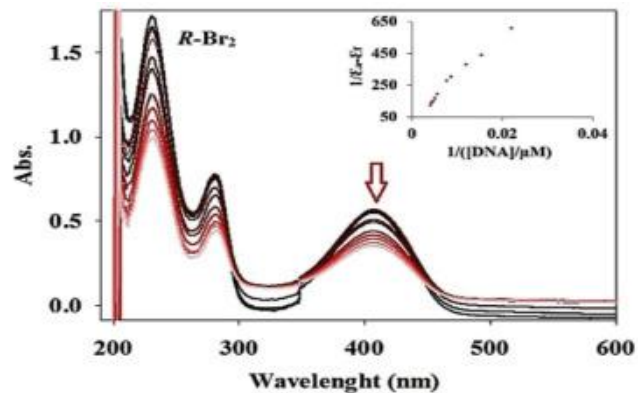
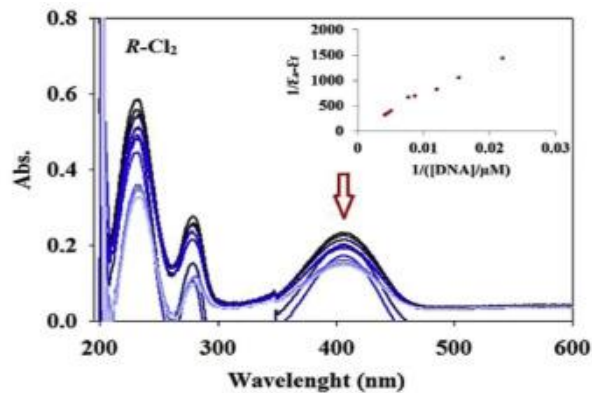


Fig. 4. UV absorption spectra of synthesized *R,S*-enantiomers in the presence of various amounts of DNA.

To quantitatively evaluate the affinity of the ligands with FS-DNA, the intrinsic binding constant  $K_b$  was determined by monitoring the changes in absorbance using the following equation [39]:

$$\frac{[DNA]}{(\varepsilon_a - \varepsilon_f)} = \frac{[DNA]}{(\varepsilon_b - \varepsilon_f)} + \frac{1}{K_b(\varepsilon_b - \varepsilon_f)} \quad (1)$$

Here, [DNA] is the concentration of DNA in base pairs.  $\varepsilon_a$ ,  $\varepsilon_f$  and  $\varepsilon_b$  are the apparent extinction coefficient, the extinction coefficient for free compounds and the extinction coefficient for the compounds in fully bound form, respectively.  $\varepsilon_f$  was determined by calibration curve and  $\varepsilon_a$  is the ratio of  $A_{obs}$  to [compound]. A plot of  $[DNA]/(\varepsilon_a - \varepsilon_f)$  vs. [DNA] gives  $K_b$  as ratio of slope to y-intercept [39].

The binding constants of FS-DNA and the synthesized ligands are given in Table 2. The

higher  $K_b$  values for ***R* ClBr** and ***S* ClBr** compared to others, shows that the binding of these 2 compounds are stronger.

Table 2. DNA-binding constant ( $K_b$ ), Stern-Volmer constant ( $K_{sv}$ ) of the compounds and quenching rate constant of DNA ( $k_q$ ).

Type of compounds		$K_b/M^{-1}$ (Fluorescence)	$K_b/M^{-1}$ (UV-Vis)	$K_{sv}/M^{-1}$	$k_q/M^{-1}S^{-1}$
<i>R</i>	Cl <sub>2</sub>	$7.66 \times 10^4$	$1.57 \times 10^3$	$4.1 \times 10^3$	$4.1 \times 10^{11}$
<i>R</i>	Br <sub>2</sub>	$4.25 \times 10^4$	$1.50 \times 10^3$	$3.8 \times 10^3$	$3.8 \times 10^{11}$
<i>R</i>	ClBr	$7.77 \times 10^4$	$1.74 \times 10^3$	$4.2 \times 10^3$	$4.2 \times 10^{11}$
<i>R</i>	I <sub>2</sub>	$3.89 \times 10^4$	$9.22 \times 10^2$	$3.0 \times 10^3$	$3.0 \times 10^{11}$
<i>S</i>	Cl <sub>2</sub>	$2.75 \times 10^4$	$2.39 \times 10^3$	$2.2 \times 10^3$	$2.2 \times 10^{11}$
<i>S</i>	Br <sub>2</sub>	$1.98 \times 10^4$	$2.37 \times 10^3$	$2.5 \times 10^3$	$2.5 \times 10^{11}$
<i>S</i>	ClBr	$2.85 \times 10^4$	$2.77 \times 10^3$	$2.0 \times 10^3$	$2.0 \times 10^{11}$



Type of compounds	$K_b/M^{-1}$ (Fluorescence)	$K_b/M^{-1}$ (UV-Vis)	$K_{sv}/M^{-1}$	$k_q/M^{-1}S^{-1}$
S I <sub>2</sub>	$1.96 \times 10^4$	$2.14 \times 10^3$	$2.5 \times 10^3$	$2.5 \times 10^{11}$

Although the electronic absorption studies have confirmed that these eight ligands can bind to DNA, it is necessary to carry out other experiments to prove the binding mode.

### 3.2.2. Competitive studies with ethidium bromide

Ethidium bromide (EtBr) fluorescence displacement experiments were used to further investigate the interaction mode between the ligands and DNA. EtBr does not show any appreciable emission in solution, which is due to fluorescence quenching of free EtBr by solvent molecules. However, in the presence of DNA, it exhibits intense fluorescence because of the intercalation to base pairs in DNA [7,40]. Addition of a second molecule to DNA can quench the DNA-induced EtBr emission, at least partially, which can prove the binding of ligands to DNA [39,41].

The competitive DNA binding of the ligands was studied by monitoring changes in the emission intensity of DNA- EtBr as a function of the ligands concentration. The emission spectra of EtBr bound to DNA in the absence and presence of these ligands are shown in Fig. 5. Upon addition of ligands to DNA pretreated with EtBr, an appreciable reduction in the DNA-induced emission intensity of EtBr is caused, indicating the interaction of the ligands with DNA. Dynamic quenching and static quenching are two different mechanisms of fluorescence quenching. Diffusion phenomenon caused dynamic quenching and formation of non-fluorescent ground state ligand caused static quenching [42]. The fluorescence quenching of DNA is described by Stern-Volmer relation [43]:

$$\frac{F_0}{F} = 1 + K_{sv} [Q] = 1 + k_q \tau [Q] \quad (2)$$

Where  $F_0$  and  $F$  represent the relative fluorescence intensities in the absence and the presence of the ligands, respectively.  $K_{sv}$  is Stern–Volmer constant and  $[Q]$  is the concentration of the quencher that quencher is the synthesized ligands here.  $k_q$  is quenching rate constant and  $\tau_0$  is the fluorescence lifetime of the bio macromolecules in the absence of quencher [9]. In consequence of fluorescence quenching of DNA,  $K_{sv}$  value calculated from the slope of plot of  $F_0/F$  versus  $[Q]$ .

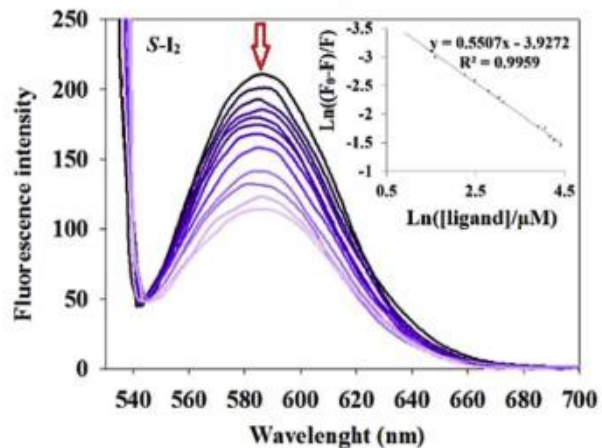
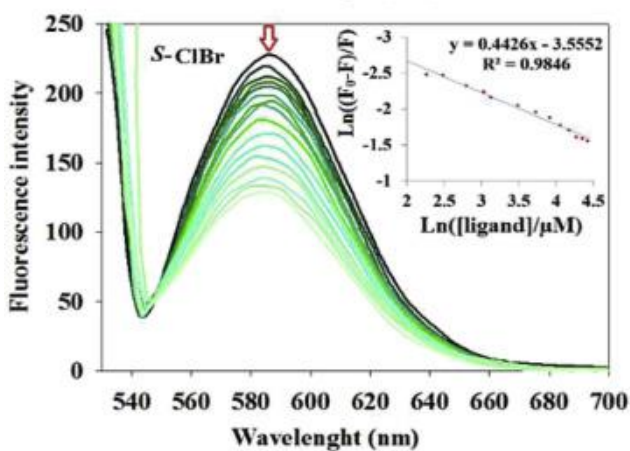
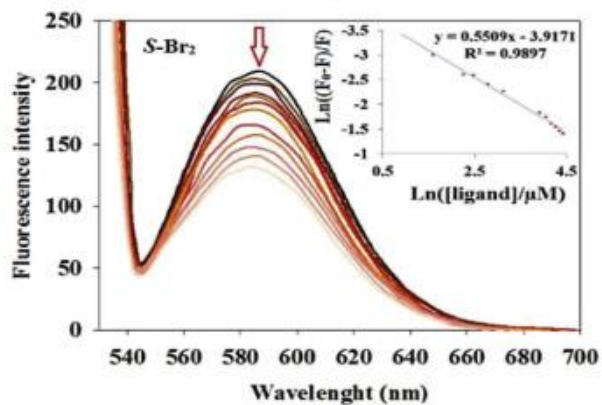
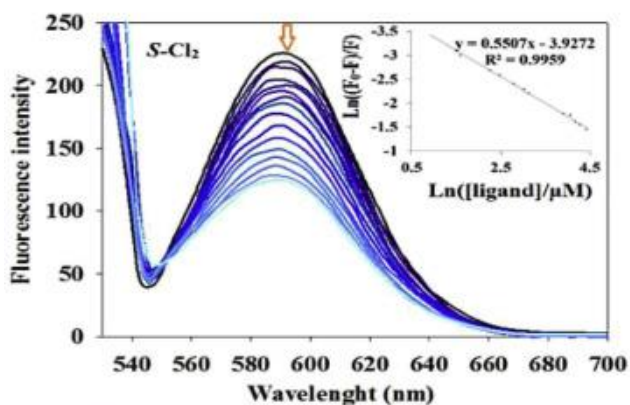
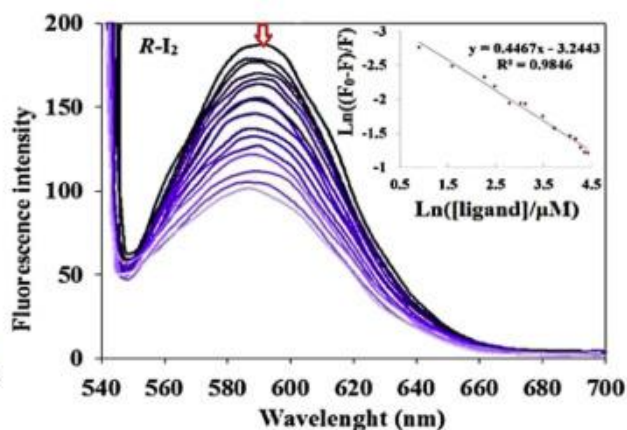
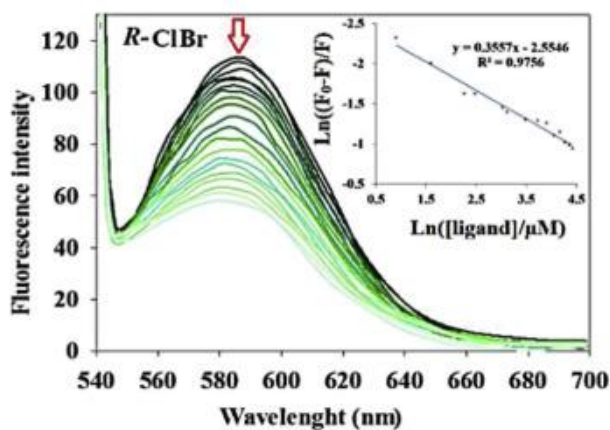
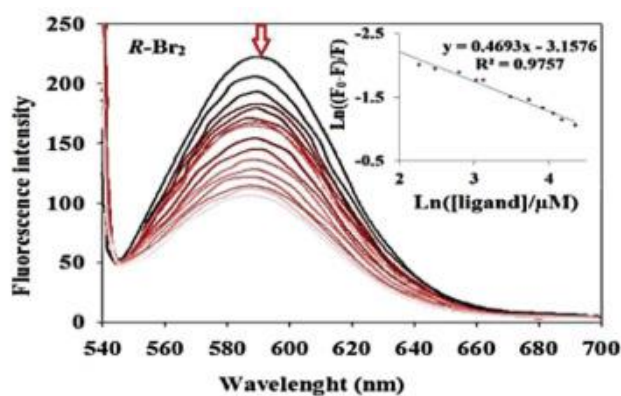
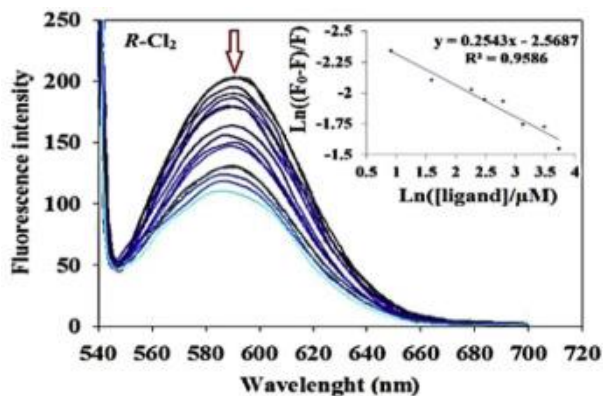


Fig. 5. Fluorescence emission spectra of ethidium bromide-DNA system in the presence of various amounts of *R,S*-enantiomers.

As a result,  $K_{sv}$  and  $k_q$  are calculated for these ligands. The values of  $k_q$  are larger than collision quenching constant ( $2 \times 10^{10} \text{ M}^{-1}\text{S}^{-1}$ ) of various quenchers with the bio macromolecules. This observation supports that quenching fluorescence of DNA occurs by static mechanism.

Moreover, binding constant ( $K_b$ ) of the ligands and FS-DNA can be calculated by this experiment using following equation [44]:

$$\ln \left( \frac{F_0 - F}{F} \right) = \ln K_b + n \ln [Q] \quad (3)$$

“ $K_b$ ” is obtained from the plot of  $\text{Ln} ((F_0 - F)/F)$  versus  $\text{Ln} [Q]$  as a y-intercept. Furthermore, “ $n$ ” which is the number of binding site per nucleic acid is slope of the plot. The  $k_q$ ,  $K_{sv}$  and  $K_b$  values for all synthesized compounds are shown in Table 2. As can be seen UV-Vis and fluorescence techniques show the same trend for  $K_b$  between all compounds and DNA.

### 3.2.3. *Molecular docking with DNA*

To gain further insight into the nature of DNA binding of the synthesized ligands, Molecular docking studies were carried out. The docked model results suggest that all ligands bind in the minor groove of DNA. The binding mode and the nucleotides around each of synthesized ligands, docking poses of ligands DNA and participant nucleotides in H-bond are presented in Table 3. Moreover, the standard binding free energies ( $\Delta G^\circ$ ), describing the affinity of the ligands for

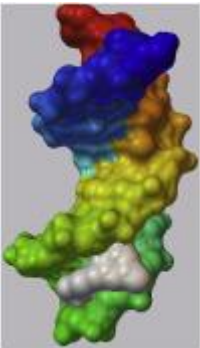
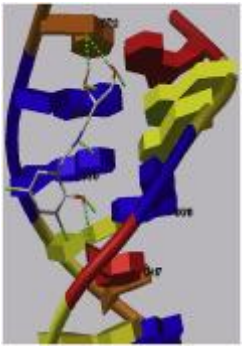
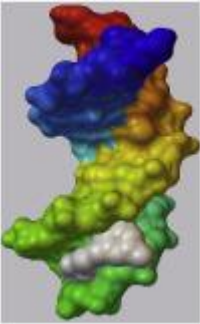
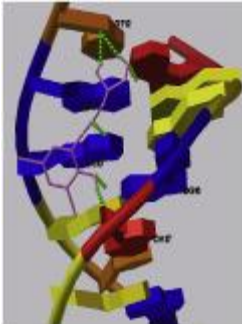
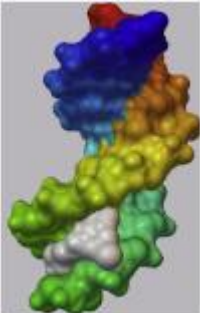
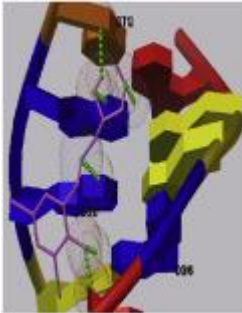
binding to DNA with the best scores, are given in Table 3. The ligand **R C1Br** is found to have higher binding affinity than its analog and the order of binding efficiency is as follows: (**R C1Br**) >

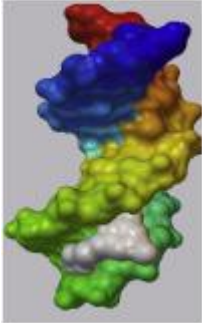
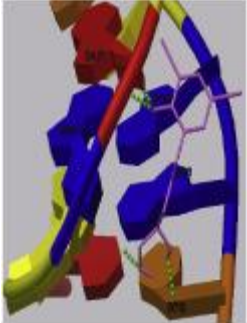
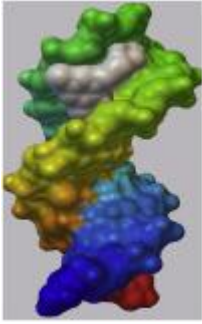
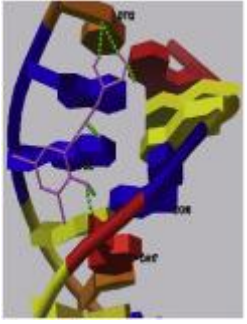
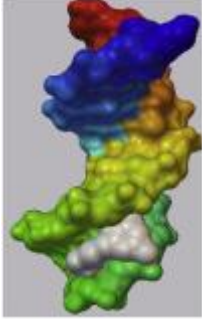
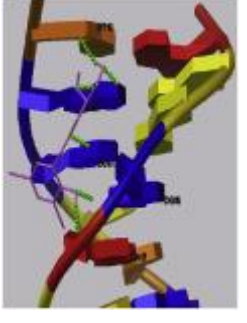
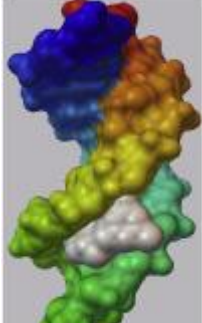
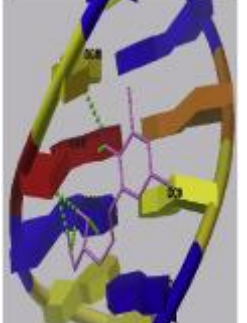
(**R C12**) > (**R Br2**) > (**R I2**). It is interesting to note that the binding energy of

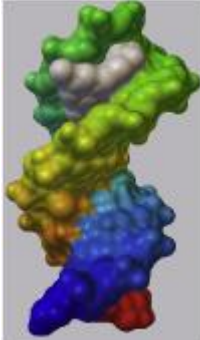
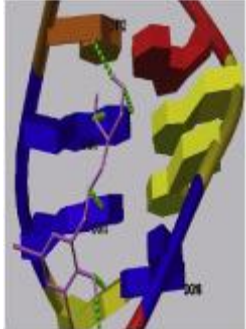
ligand **S C1Br** is more than that of its analog and the order of binding efficiency is as follows:

(**S C1Br**) > (**S C12**) > (**S Br2**) > (**S I2**). These results are the same as the obtained results from experimental methods. Thus, our molecular modeling studies throw light on the binding modes by which these compounds interact with DNA and complement the experimental observations.

Table 3. Molecular docking Results for the interaction of ligands with DNA.

Type of compounds	Bases around ligand	Number of Hydrogen bond	Binding Energy/kcal.mol <sup>-1</sup>	Binding site	Zoom out (Conformation of complex in binding site)
<i>R</i>	Cl <sub>2</sub>	DG10 DG11 DG16 DA17 DT12	7 -6.3		
<i>R</i>	Br <sub>2</sub>	DG10 DG11 DG16 DA17 DT12	6 -6.08		
<i>R</i>	ClBr	DG10 DG11 DG16 DA17 DT12	6 -6.34		

Type of compounds	Bases around ligand	Number of Hydrogen bond	Binding Energy/kcal.mol <sup>-1</sup>	Binding site	Zoom out (Conformation of complex in binding site)
<i>R</i>	I <sub>2</sub>	DG11 DG16 DA17 DT12	4	-5.45	 
<i>S</i>	Cl <sub>2</sub>	DG10 DG11 DG16 DA17 DT12	6	-5.51	 
<i>S</i>	Br <sub>2</sub>	DG10 DG11 DG16 DA17 DT12	6	-5.26	 
<i>S</i>	ClBr	DG16 DA17 DC18	6	-5.99	 

Type of compounds	Bases around ligand	Number of Hydrogen bond	Binding Energy/kcal.mol <sup>-1</sup>	Binding site	Zoom out (Conformation of complex in binding site)
<i>S</i>	<i>I</i> <sub>2</sub>	DG10 DG11 DG16 DA17 DT12	6 -5.19		

In this study, Molecular docking was used to investigate existence halogen bond in the ligand-DNA complexes. Also the angles and distances of bonds have been measured by this program. Results for geometry of each halogen bond are shown in Table 4. Halogen bonds can be formed between a halogenated ligand and any accessible Lewis base in the binding pocket. This bond is observed in cysteine, methionine, serine, glutamate, tryptophan etc. [45]. Therefore, the existence of halogen bond between the synthesized compounds and DNA is possible and molecular docking also confirms it. It is noteworthy that inserting bulk groups like halogens into organic molecules can lead to increase binding affinity, membrane permeability and therefore, improve the oral absorption. Since bulk groups tend to occupy all the active site of molecular targets, including the deeper pockets [46].

Table 4. Molecular docking results for the halogen bond between the ligands and DNA.

Type of compounds	C-X ... Y	base pair	X...Y distance (Å)	C-X...Y angle (deg)
<i>R</i>	ClBr	C Cl...O	DG-11 3.410	129.48
		C Br...N	DA17 3.369	132.818
<i>R</i>	Cl <sub>2</sub>	C Cl(5) ... O	DG10 3.486	120.038
		C Cl(3) ... O	DA17 3.806	87.459
		C Cl(3) ... N	DA17 3.373	150.031

Type of compounds		C-X ... Y	base pair	X...Y distance (Å)	C-X...Y angle (deg)	
<i>R</i>	Br <sub>2</sub>	C	Br(5) ... O	DG11	3.426	123.636
		C	Br(3) ... O	DA17	3.611	86.155
		C	Br(3) ... N	DA17	3.311	144.936
<i>R</i>	I <sub>2</sub>	C	I(5) ... O	DG10	3.370	109.731
		C	I(3) ... N	DA17	3.573	134.360
<i>S</i>	ClBr	C	Cl...O	DC9	2.949	113.660
		C	Br...O	DC18	3.073	127.717
		C	Br...O	DA17	3.428	98.644
<i>S</i>	Cl <sub>2</sub>	C	Cl(5) ... O	DG10	2.827	106.926
		C	Cl(3) ... O	DA17	3.537	87.282
		C	Cl(3) ... N	DA17	3.098	147.819
<i>S</i>	Br <sub>2</sub>	C	Br(3) ... N	DA17	3.474	141.821
<i>S</i>	I <sub>2</sub>	C	I(3) ... O	DA17	3.878	75.381
		C	I(3) ... N	DA17	3.489	133.100

For example, Fig. 6 shows halogen bonding interaction between *S*-**Cl<sub>2</sub>** and DNA. Three types

of bonds between this ligand and DNA is clearly observed (H-bond, X-bond and hX-bond). There are six hydrogen bonds in the ligand and DNA complex and we can see three halogen bonds with identified and admissible geometric parameters. Interaction between Cl at position 5 and

oxygen of DG10 is one of the bonds,  $(d(\text{Cl}\cdots\text{O})) = 2.82 \text{ \AA}$ ,  $(\angle \text{C}-\text{Cl}\cdots\text{O}) = 106.9^\circ$ . Remarkably, in some cases, there are multiple halogen bonding interaction. For instance, in this ligand, the Cl atom at position 3 is involved in two halogen bond with N and O of DA17 ( $d(\text{Cl}\cdots\text{N}) = 3.098 \text{ \AA}$ ,

$(\angle \text{C}-\text{Cl}\cdots\text{N}) = 147.8^\circ$ ;  $(d(\text{Cl}\cdots\text{O})) = 3.537 \text{ \AA}$ ,  $(\angle \text{C}-\text{Cl}\cdots\text{O}) = 87.2^\circ$  respectively. Latter case is

hX-bond. In this type of bonding, H-bond and X-bonds can compete or complement each other and geometrically are perpendicular to each other. So  $\Theta_1 = 87.2^\circ$  is reasonable for this case but about other cases  $\Theta_1$  value should be close to  $160^\circ$ . We can see strength of a halogen bond depends on X...Y distance (Table 4). The obtained data from molecular docking for X-bonds in the ligand-DNA complexes which are presented in Table 4, show that X...Y distances are followed as: (**R**-

**ClBr**)  $\approx$  (**R**-**Cl<sub>2</sub>**) > (**R**-**Br<sub>2</sub>**) > (**R**-**I<sub>2</sub>**) and (**S**-**ClBr**)  $\approx$  (**S**-**Cl<sub>2</sub>**) > (**R**-

**Br<sub>2</sub>**)  $\approx$  (**S**-**I<sub>2</sub>**). Interestingly, calculated DNA-binding constants of these ligands using experimental methods are in the same order. In other words, this can be concluded that binding affinity of the ligands to DNA depends on strength of halogen bonds. Fig. S25 shows halogen and hydrogen bonding interaction between other ligands and DNA.

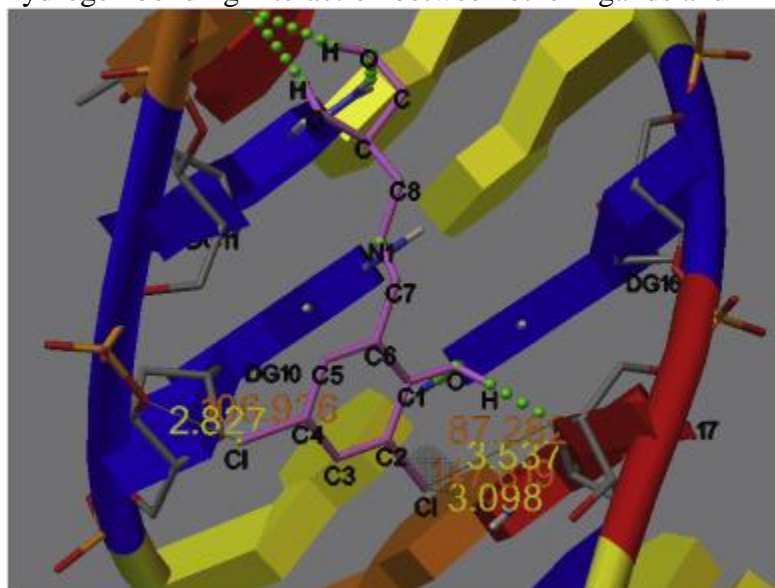


Fig. 6. Illustration of a halogen bond in a DNA-*S*-**Cl<sub>2</sub>**. Chlorine forms a halogen bond with oxygen and nitrogen of the DNA. The ligand is shown as a pink stick model and DNA is shown as both a cartoon and stick model. Small green spheres show H-bond interaction. The image was



prepared using AutoDock. (For interpretation of the references to colour in this figure legend, the reader is referred to the Web version of this article.)

### 3.3. Anticancer activity of compounds

Investigation of anticancer effects of the Schiff base compounds on MCF-7 and HeLa cancer cell lines (as two major and prevalent cancer types) using MTT assay clearly showed their dose- and cell line-dependent anticancer activity. The compounds displayed higher anticancer activity on HeLa cells than MCF-7 cells and the effects significantly increased in higher concentrations of the compounds (Fig. 7, Fig. 8). Moreover, the results interestingly indicated that the anticancer activity is significantly dependent on the chirality of Schiff base compounds as **R** compounds displayed significantly higher anticancer activity than **S** compounds.

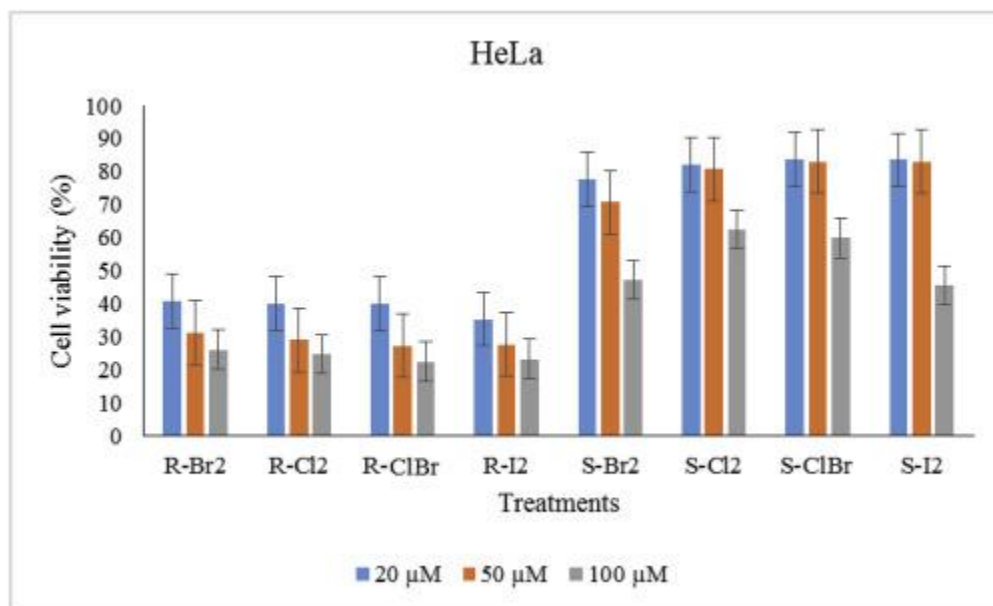


Fig. 7. The viability percentage of HeLa cancer cells after 48 h incubation with different concentrations of the Schiff base compounds.

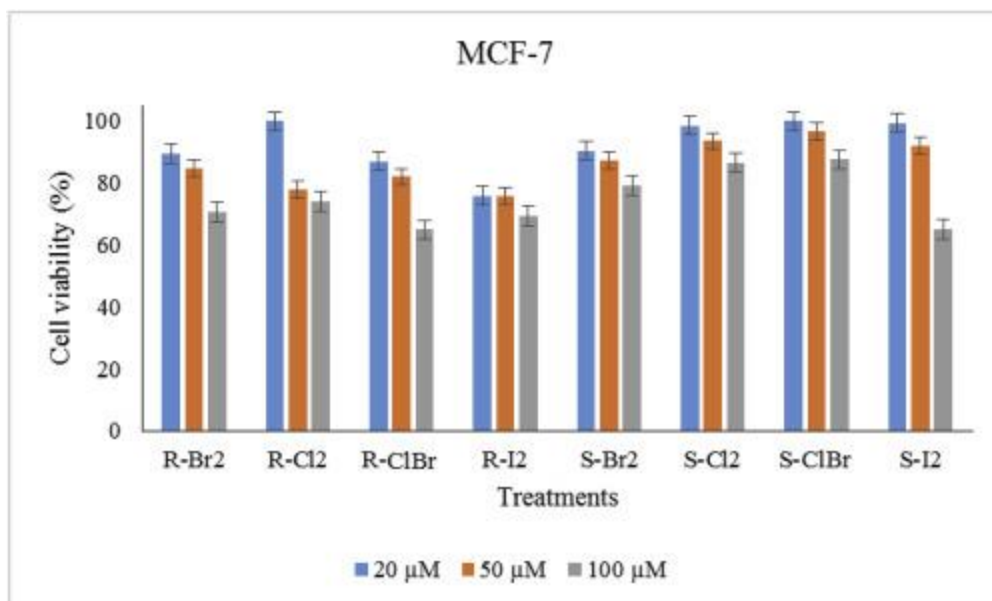


Fig. 8. The viability percentage of MCF-7 cancer cells after 48 h incubation with different concentrations of the Schiff base compounds.

Based on the results, more than 75% mortality obtained after 48 h exposure of HeLa cancer cells to 100 μM concentration of **R** enantiomers (Fig. 7). It would be mentioned that up to 65% mortality was also observed at the same conditions with addition of lower concentration (20 μM) of these enantiomers. At the same conditions, the maximum mortality of HeLa cancer cells in the presence

of **S** enantiomers was (64.42%) that obtained after 48 h exposure to 100 μM **S I<sub>2</sub>** compound (Fig. 7).

MCF-7 cells showed less sensitivity to these compounds than HeLa cell line as maximum mortality

of 35.15% obtained at the same conditions by using 100 μM **R ClBr**. The anticancer effects of **S** enantiomers on MCF-7 cells was relatively less than **R** enantiomers (Fig. 8).

The microscopic monitoring of cell morphology, in accordance with the results of MTT assays, showed different levels of cytotoxicity based on the cell line and chirality of Schiff base compounds (Fig. 9, Fig. 10). The significant differences regarding to cell morphology could be clearly seen between the cells exposed to different compounds. The cell shrinkage and rounding, as primary signs of cell death, could be clearly observed in the treated cells. The significantly reduced cell density after 48 h treatment in comparison with the control cells may be attributed to the inhibition of cell growth or cell death due to the exposure to compounds. The afore mentioned changes were considerably less in MCF-7 cells (Fig. 9) than HeLa cells (Fig. 10) which confirmed the results of MTT assays. The overall results indicate that these Schiff base compounds especially **R** enantiomers have great potential for development of anticancer agents.

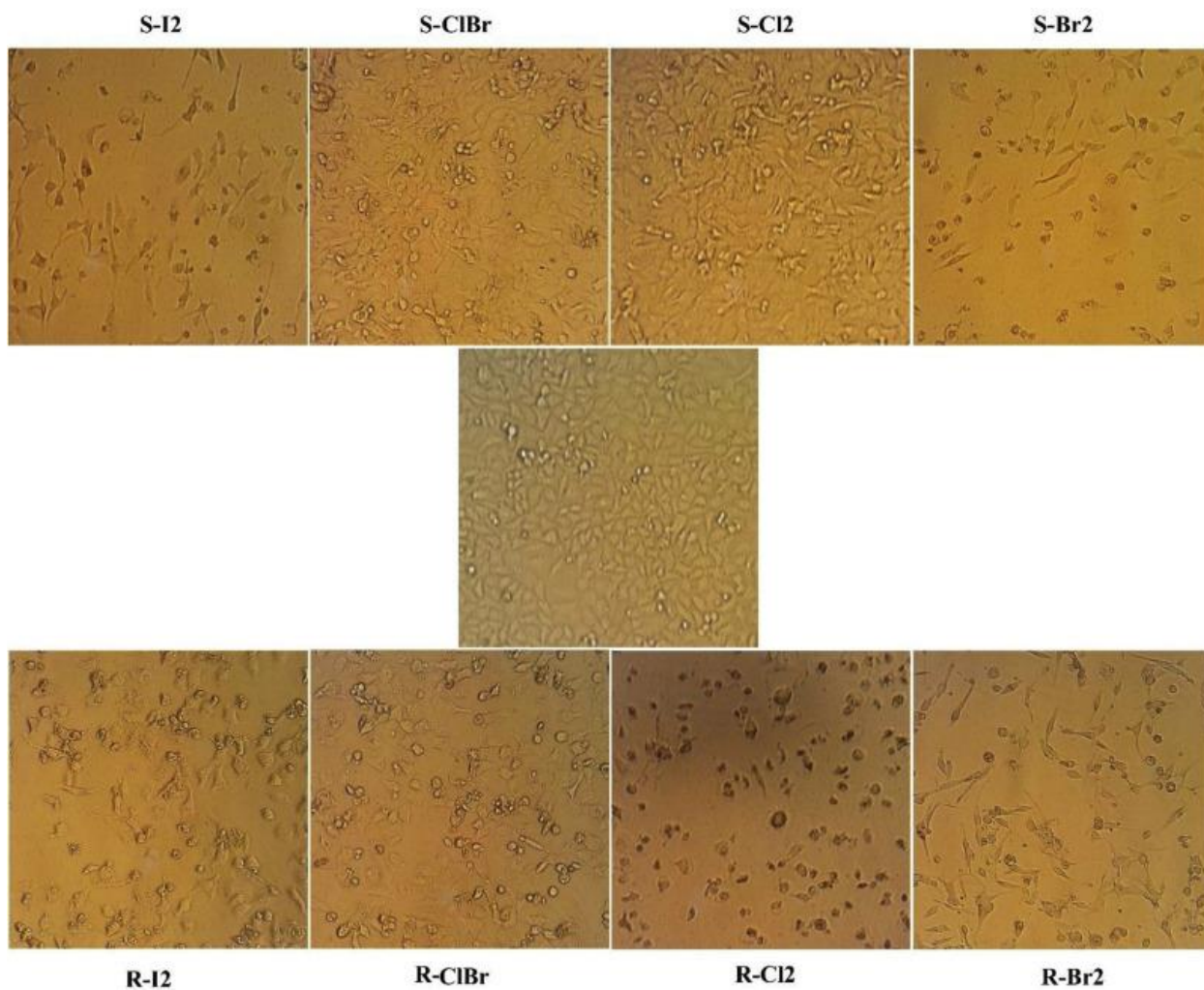


Fig. 9. Morphological changes of MCF-7 cancer cells after 48 h incubation with the Schiff base compounds. The middle figure represents the control cells without treatment.

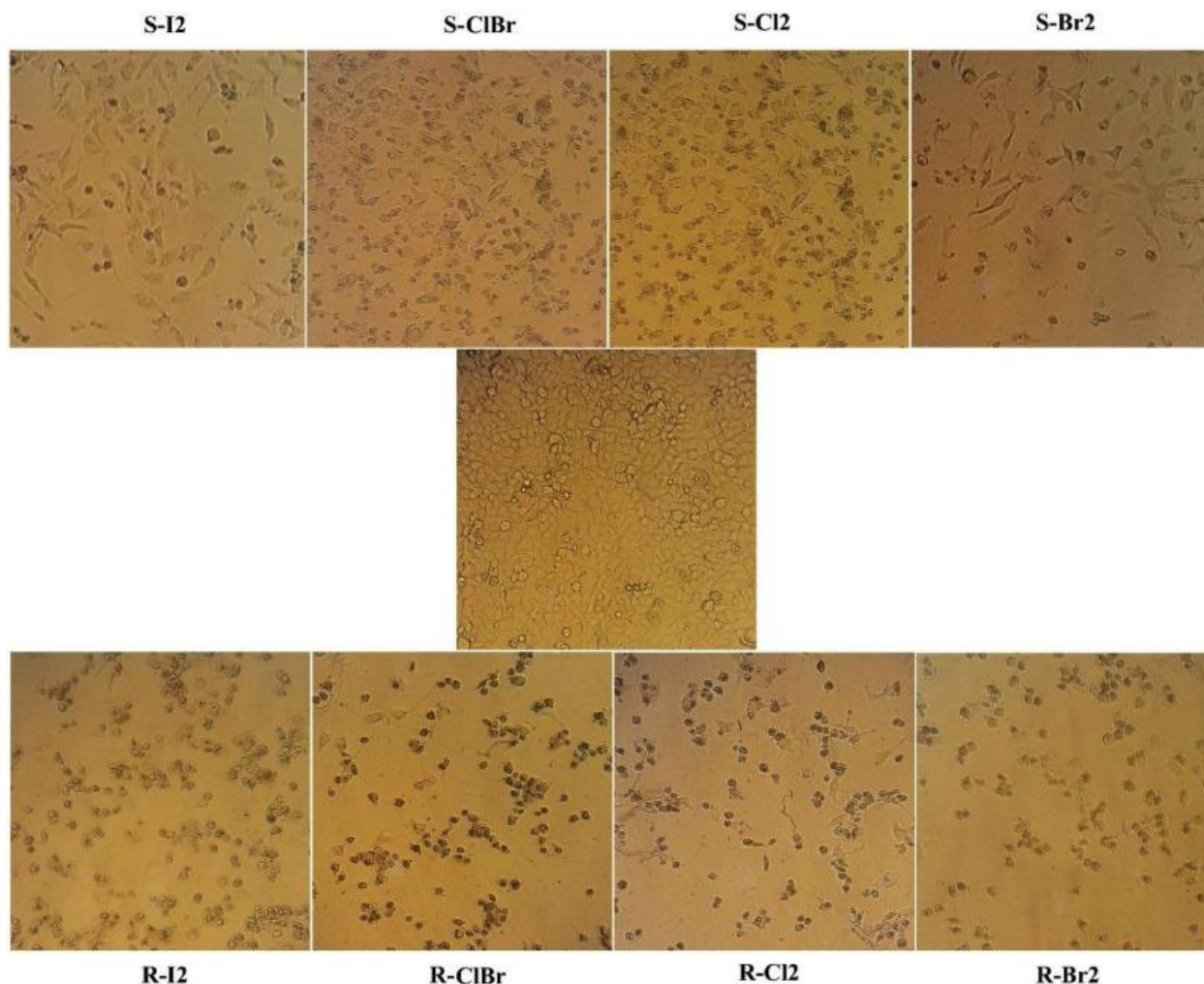


Fig. 10. Morphological changes of HeLa cancer cells after 48 h incubation with the Schiff base compounds. The middle figure represents the control cells without treatment.

#### 4. Conclusion

In summary, we have synthesized eight novel chiral halogenated Schiff base ligands. They were characterized by FT-IR, circular dichroism (CD), elemental analysis (CHN),  $^1\text{H}$  NMR and  $^{13}\text{C}$  NMR spectroscopies. Herein, we compared biological activities of two enantiomers, *R*-L and *S*-L. In addition, the effect of halogen atoms on their activities was evaluated. The experimental (fluorescence quenching and UV-vis spectroscopy) and computational methods (molecular docking) were used to study DNA-binding of the ligands. The obtained results indicate that the ligands bind to DNA as: (*R* ClBr) > (*R* Cl<sub>2</sub>) > (*R* Br<sub>2</sub>) > (*R* I<sub>2</sub>) and (*S* ClBr) > (*S* Cl<sub>2</sub>) > (*S* Br<sub>2</sub>) > (*S* I<sub>2</sub>). The ligands can form halogen bonds with DNA that were confirmed by molecular docking. This method was also measured the bond distances

and bond angles. The study of obtained data have concluded that binding affinity of the ligands to DNA depends on strength of halogen bonds.

The anticancer activity of the ligands on HeLa and MCF-7 was investigated and the results indicate that these ligands especially *R* enantiomers have great potential for development of anticancer agents.

## Appendix A. Supplementary data

Supplementary data related to this article can be found at <https://doi.org/10.1016/j.molstruc.2018.02.042>.

### References

- [1] M. Carreira, R. Calvo-Sanjuán, M. Sanaú, X. Zhao, R.S. Magliozzo, I. Marzo, M. Contel, Cytotoxic hydrophilic iminophosphorane coordination compounds of d8 metals. Studies of their interactions with DNA and HSA, *J. Inorg. Biochem.* 116 (2012) 204e214.
- [2] L. Yan, X. Wang, Y. Wang, Y. Zhang, Y. Li, Z. Guo, Cytotoxic palladium(II) complexes of 8-aminoquinoline derivatives and the interaction with human serum albumin, *J. Inorg. Biochem.* 106 (2012) 46e51.
- [3] Z. Shokohi-Pour, H. Chiniforoshan, M.R. Sabzalian, S.A. Esmaeili, A.A. Momtaziborjani, Cobalt (II) complex with novel unsymmetrical tetradentate Schiff base (ON) ligand: in vitro cytotoxicity studies of complex, interaction with DNA/protein, molecular docking studies, and antibacterial activity, *J. Biomol. Struct. Dyn.* 36 (2) (2018) 532e549.
- [4] Z.H. Chohan, S.H. Sumrra, M.H. Youssoufi, T.B. Hadda, Metal based biologically active compounds: design, synthesis, and antibacterial/antifungal/cytotoxic properties of triazole-derived Schiff bases and their oxovanadium (IV) complexes, *Eur. J. Med. Chem.* 45 (7) (2010) 2739e2747.
- [5] P. Ghorai, R. Saha, S. Bhuiya, S. Das, P. Brandão, D. Ghosh, T. Bhaumik, P. Bandyopadhyay, D. Chattopadhyay, A. Saha, Syntheses of Zn (II) and Cu (II) Schiff base complexes using N, O donor Schiff base ligand: crystal structure, DNA binding, DNA cleavage, docking and DFT study, *Polyhedron* 141 (2018) 153e163.
- [6] Z. Kazemi, H. Amiri Rudbari, M. Sahihi, V. Mirkhani, M. Moghadam, S. Tangestaninejad, I. Mohammadpoor-Baltork, S. Gharaghani, Synthesis, characterization and biological application of four novel metal-Schiff base complexes derived from allylamine and their interactions with human serum albumin: experimental, molecular docking and ONIOM computational study, *J. Photochem. Photobiol. A* 162 (2016) 448e462.
- [7] D.N. Akbayeva, L. Gonsalvi, W. Oberhauser, M. Peruzzini, F. Vizza, P. Brüggeller, A. Romerosa, G. Sava, A. Bergamo, Synthesis, catalytic properties and biological activity of new water soluble ruthenium cyclopentadienyl PTA complexes [(C<sub>5</sub>R<sub>5</sub>)RuCl(PTA)<sub>2</sub>](R<sup>1/4</sup>H, Me; PTA<sup>1/4</sup> 1, 3, 5-triaza-7-phosphaadamantane), *ChemComm.* 2 (2003) 264e265.
- [8] R. del Campo, J.J. Criado, E. Garcí

a, M.a.R. Hermosa, A. Jimenez-Sanchez,

- J.L. Manzano, E. Monte, E. Rodriguez-Fernandez, F. Sanz, Thiourea derivatives and their nickel (II) and platinum (II) complexes: antifungal activity, *J. Inorg. Biochem.* 89 (1) (2002) 74e82.
- [9] F. Arjmand, M. Muddassir, R.H. Khan, Chiral preference of l-tryptophan derived metal-based antitumor agent of late 3d-metal ions (Co (II), Cu (II) and Zn (II)) in comparison to d-and dl-tryptophan analogues: their in vitro reactivity towards CT DNA, 50-GMP and 50-TMP, *Eur. J. Med. Chem.* 45 (9) (2010) 3549e3557.
- [10] R. Vijayalakshmi, M. Kanthimathi, R. Parthasarathi, B.U. Nair, Interaction of chromium (III) complex of chiral binaphthyl tetradentate ligand with DNA, *Bioorg. Med. Chem.* 14 (10) (2006) 3300e3306.
- [11] Y. Lu, Y. Wang, W. Zhu, Nonbonding interactions of organic halogens in biological systems: implications for drug discovery and biomolecular design, *Phys. Chem. Chem. Phys.* 12 (18) (2010) 4543e4551.
- [12] G.R. Desiraju, P.S. Ho, L. Kloo, A.C. Legon, R. Marquardt, P. Metrangolo, P. Politzer, G. Resnati, K. Rissanen, Definition of the halogen bond (IUPAC Recommendations 2013), *Pure Appl. Chem.* 85 (8) (2013) 1711e1713.
- [13] Z. Xu, Z. Yang, Y. Liu, Y. Lu, K. Chen, W. Zhu, Halogen bond: its role beyond drugtarget binding affinity for drug discovery and development, *J. Chem. Inf. Model.* 54 (1) (2014) 69e78.
- [14] T.T. Tidwell, Hugo (Ugo) schiff, schiff bases, and a century of b-lactam synthesis, *Angew. Chem. Int. Ed.* 47 (6) (2008) 1016e1020.
- [15] R.W. Layer, The chemistry of imines, *Chem. Rev.* 63 (5) (1963) 489e510.
- [16] E.D. Cross, U.A. Shehzad, S.M. Lloy, A.R. Brown, T.D. Mercer, D.R. Foster, B.L. McLellan, A.R. Murray, M.A. English, M. Bierenstiel, Synthesis and characterization of donor-functionalized N, S-Compounds containing the orthoaminothiophenol motif, *Synthesis* 2011 (02) (2011) 303e315.
- [17] A. Xavier, N. Srividhya, Synthesis and study of Schiff base ligands, *IOSR J. Appl. Chem.* 7 (2014) 06e15.
- [18] M. Jayandran, M. Haneefa, V. Balasubramanian, Synthesis, characterization and biological activities of turmeric curcumin schiff base complex, *Int. J. Chem. Nat. Sci.* 2 (5) (2014) 157e163.
- [19] S. Bhagat, N. Sharma, T.S. Chundawat, Synthesis of some salicylaldehydebased Schiff bases in aqueous media, *J. Chem.* 2013 (2012).
- [20] M. Zarei, A. Jarrahpour, Green and efficient synthesis of azo Schiff bases, *Iran. J. Sci. Technol.* 35 (3) (2011) 235e242.
- [21] R.K. Koiri, S.K. Trigun, S.K. Dubey, S. Singh, L. Mishra, Metal Cu (II) and Zn (II) bipyridyls as inhibitors of lactate dehydrogenase, *Biometals* 21 (2) (2008) 117e126.
- [22] R.A. Gaussian09, 1, MJ Frisch, GW Trucks, HB Schlegel, GE Scuseria, MA Robb, JR Cheeseman, G. Scalmani, V. Barone, B. Mennucci, GA Petersson et al., Gaussian, Inc., Wallingford CT, (2009).
- [23] F. Arjmand, M. Muddassir, A mechanistic approach for the DNA binding of chiral enantiomeric L-and D-tryptophan-derived metal complexes of 1, 2-DACH: cleavage and antitumor activity, *Chirality* 23 (3) (2011) 250e259.
- [24] J.D. Chellaian, J. Johnson, Spectral characterization, electrochemical and anticancer

- studies on some metal (II) complexes containing tridentate quinoxaline Schiff base, *Spectrochim. Acta* 127 (2014) 396e404.
- [25] A.A. Kajani, A.-K. Bordbar, S.H.Z. Esfahani, A. Razmjou, Gold nanoparticles as potent anticancer agent: green synthesis, characterization, and in vitro study, *RSC Adv.* 6 (68) (2016) 63973e63983.
- [26] Z. Kazemi, H. Amiri Rudbari, M. Sahihi, V. Mirkhani, M. Moghadam, S. Tangestaninejad, I. Mohammadpoor-Baltork, G. Azimi, S. Gharaghani, A.A. Kajani, Synthesis, characterization and separation of chiral and achiral diastereomers of Schiff base Pd (II) complex: a comparative study of their DNA-and HSA-binding, *Photochem. Photobiol.* 163 (2016) 246e260.
- [27] L. L\_ az\_ ar, A. Gēoblyēos, T.A. Martinek, F. Fūlfop, Ring\_ chain tautomerism of 2-aryl-substituted cis-and trans-decahydroquinazolines, *J. Org. Chem.* 67 (14) (2002) 4734e4741.
- [28] M.S. Bharara, K. Strawbridge, J.Z. Vilsek, T.H. Bray, A.E. Gordon, Novel dinuclear uranyl complexes with asymmetric Schiff base ligands: synthesis, structural characterization, reactivity, and extraction studies, *Inorg. Chem.* 46 (20) (2007) 8309e8315.
- [29] N. Berova, K. Nakanishi, R.W. Woody, *Circular Dichroism Principles and Applications*, second ed., John Wiley & Sons, 2000.
- [30] H. Amouri, M. Gruselle, *Chirality in Transition Metal Chemistry: Molecules, Supramolecular Assemblies and Materials*, first ed., vol. 33, John Wiley & Sons, 2008.
- [31] D.P. Demarque, C. Merten, Intra-versus intermolecular hydrogen bonding: solvent-dependent conformational preferences of a common supramolecular binding motif from 1H NMR and vibrational circular dichroism spectra, *Chem. Eur J.* 23 (71) (2017) 17915e17922.
- [32] V.M. Demyanovich, I. N. Shishkina, N.S. Zefirov, Effect of intramolecular interactions on circular dichroism of ortho-substituted 1-phenethylamines, *Chirality* 16 (8) (2004) 486e492.
- [33] Y. Iwasaki, M. Kimura, A. Yamada, Y. Mutoh, M. Tateishi, H. Arai, Y. Kitamura, M. Chikira, Conformational change of ternary copper (II) complexes of cationic Schiff-bases and N-heteroaromatic amines induced by intercalative binding to DNA, *Inorg. Chem. Commun.* 14 (9) (2011) 1461e1464.
- [34] A. Terenzi, G. Barone, A. Silvestri, A.M. Giuliani, A. Ruggirello, V.T. Liveri, The interaction of native calf thymus DNA with Fe III-dipyrido [3, 2-a: 2', 3'-c] phenazine, *J. Inorg. Biochem.* 103 (1) (2009) 1e9.
- [35] Y. Xing, W. Zhang, J. Song, Y. Zhang, X. Jiang, R. Wang, Anticancer effects of a novel class rosin-derivatives with different mechanisms, *Bioorg. Med. Chem. Lett* 23 (13) (2013) 3868e3872.
- [36] F. Darabi, H. Hadadzadeh, M. Ebrahimi, T. Khayamian, H. Amiri Rudbari, The piroxicam complex of cobalt (II): synthesis in two different ionic liquids, structure, DNA-and BSA interaction and molecular modeling, *Inorg. Chim. Acta.* 409 (2014) 379e389.
- [37] Z. Kazemi, H. Amiri Rudbari, V. Mirkhani, M. Sahihi, M. Moghadam, S. Tangestaninejad, I. Mohammadpoor-Baltork, Synthesis, characterization, crystal structure, DNA-and HSA-binding studies of a dinuclear Schiff base Zn

- (II) complex derived from 2-hydroxynaphthaldehyde and 2-picolylamine, *J. Mol. Struct.* 1096 (2015) 110e120.
- [38] S. Tabassum, G.C. Sharma, A. Asim, A. Azam, R.A. Khan, Chiral nano heterobimetallic DNA receptors: in vitro binding studies, cleavage activity and DNA condensation studies (TEM and AFM imaging), *J. Organomet. Chem.* 713 (2012) 123e133.
- [39] Z. Kazemi, H. Amiri Rudbari, V. Mirkhani, M. Sahihi, M. Moghadam, S. Tangestaninejad, I. Mohammadpoor-Baltork, A.A. Kajani, G. Azimi, Selfrecognition of the racemic ligand in the formation of homochiral dinuclear V (V) complex: in vitro anticancer activity, DNA and HSA interaction, *Eur. J. Med. Chem.* 135 (2017).
- [40] X. Wang, M. Yan, Q. Wang, H. Wang, Z. Wang, J. Zhao, J. Li, Z. Zhang, In vitro DNA-binding, anti-oxidant and anticancer activity of indole-2-carboxylic acid dinuclear copper (II) complexes, *Molecules* 22 (1) (2017) 171.
- [41] M. Azam, Z. Hussain, I. Warad, S.I. Al-Resayes, M.S. Khan, M. Shakir, A. Trzesowska-Kruszynska, R. Kruszynski, Novel Pd (II)esalen complexes showing high in vitro anti-proliferative effects against human hepatoma cancer by modulating specific regulatory genes, *Dalton Trans.* 41 (35) (2012) 10854e10864.
- [42] N.-u.H. Khan, N. Pandya, K.J. Prathap, R.I. Kureshy, S.H.R. Abdi, S. Mishra, H.C. Bajaj, Chiral discrimination asserted by enantiomers of Ni (II), Cu (II) and Zn (II) Schiff base complexes in DNA binding, antioxidant and antibacterial activities, *Spectrochim. Acta* 81 (1) (2011) 199e208.
- [43] K. Hu, F. Li, Z. Zhang, F. Liang, Synthesis of two potential anticancer copper (ii) complex drugs: their crystal structure, human serum albumin/DNA binding and anticancer mechanism, *New J. Chem.* 41 (5) (2017) 2062e2072.
- [44] S.U. Dighe, S. Khan, I. Soni, P. Jain, S. Shukla, R. Yadav, P. Sen, S.M. Meeran, S. Batra, Synthesis of b-carboline-based n-heterocyclic carbenes and their antiproliferative and antimetastatic activities against human breast cancer cells, *J. Med. Chem.* 58 (8) (2015) 3485e3499.
- [45] R. Wilcken, M.O. Zimmermann, A. Lange, A.C. Joerger, F.M. Boeckler, Principles and applications of halogen bonding in medicinal chemistry and chemical biology, *J. Med. Chem.* 56 (4) (2013) 1363e1388.
- [46] M.Z. Hernandez, S.M.T. Cavalcanti, D.R.M. Moreira, J. de Azevedo, W. Filgueira, A.C.L. Leite, Halogen atoms in the modern medicinal chemistry: hints for the drug design, *Curr. Drug Targets* 11 (3) (2010) 303e314.